CT610: A Mn-Dependent Self-Sacrificing Oxygenase in *p*-Aminobenzoate Biosynthesis in *Chlamydia trachomatis*

Rowan S. Wooldridge

Thesis submitted to the faculty of the Virginia Polytechnic Institute and State University
in partial fulfillment of the requirements for the degree of

Master of Science
In
Biochemistry

Kylie D. Allen, Chair
Justin A. Lemkul
Pablo Sobrado

04/18/2022
Blacksburg, Virginia

Keywords: Self-Sacrificing enzyme, oxygenase, folate biosynthesis, *p*-aminobenzoate biosynthesis *Chlamydia trachomatis*

CT610: A Mn-Dependent Self-Sacrificing Oxygenase in *p*-Aminobenzoate Biosynthesis in *Chlamydia trachomatis*

Rowan S. Wooldridge

ABSTRACT

Folate is an essential cofactor required for several processes including DNA and amino acid biosynthesis. Folate molecules are made up of three parts: a pteridine ring, *p*-aminobenzoate (pABA), and a variable number of glutamate residues. *Chlamydia trachomatis* synthesizes folate *de novo*; however, several genes encoding enzymes required for the canonical folate biosynthesis pathway are missing, including *pabA/B* and *pabC*, which are normally required for pABA biosynthesis from chorismate. Previous studies have found that a single gene in *C. trachomatis*, CT610, functionally replaces the canonical pABA biosynthesis genes. Interestingly, CT610 does not use chorismate as a substrate. Instead, the CT610-route for pABA biosynthesis incorporates isotopically labeled tyrosine into the synthesized pABA molecule. However, *in vitro* experiments revealed that CT610 produces pABA without any added substrates (including tyrosine) in the presence of a reducing agent and molecular oxygen. CT610 shares low sequence similarity to non-heme diiron oxygenases and the previously solved crystal structure revealed a diiron active site. Taken together, CT610 is proposed to be a novel self-sacrificing enzyme that uses one of its active site tyrosine residues as a precursor to pABA in a reaction that requires O_2 and a reduced metallocofactor. Here, we discuss our progress towards understanding CT610-catalyzed pABA synthesis. Upon investigation of the pABA production and oxygenase activities of several active site tyrosine to phenylalanine variants, we found that Y27 and/or Y43 are the most likely precursors to

the resulting pABA molecule. Further, activity was nearly completely abolished with a K152R variant, suggesting that this conserved lysine may be the required amino group donor. We also developed an *in vitro* Fe(II) reconstitution procedure, where the reconstituted enzyme exhibited a drastic increase in oxygenase activity but, surprisingly, a significant decrease in pABA synthase activity. Interestingly, a significant increase in pABA synthase activity was observed when the enzyme was reconstituted with manganese as opposed to iron, suggesting that the diiron active site of this enzyme might not be directly involved in CT610-dependent production of pABA and instead Mn may be the actual cofactor. Finally, we show that two ^{18}O atoms from molecular oxygen are incorporated into the pABA molecule when synthesized by Mn-reconstituted CT610, providing further evidence for the oxygenase activity of CT610 and supporting our proposed mechanism that involves two monooxygenase reactions.

CT610: A Mn-Dependent Self-Sacrificing Oxygenase in *p*-Aminobenzoate Biosynthesis in *Chlamydia trachomatis*

Rowan S. Wooldridge

GENERAL AUDIENCE ABSTRACT

Folate is an essential molecule that is required for all cells to survive. Folate is usually made in the cell with the help from proteins known as enzymes. Enzymes help biochemical reactions happen by speeding up the rate of their specific chemical reaction. In order for this to occur, an enzyme binds to a very specific molecule, called a substrate, and facilitates the reaction transforming the substrate into a new product while not altering the enzyme in the process, allowing for the protein to continuously facilitate this reaction. *Chlamydia trachomatis* is the strain of bacteria that causes one of the most common sexually transmitted infections in the US, Chlamydia. These bacteria make folate themselves but have been shown to make this molecule in a very different way from an average folate-synthesizing organism. One enzyme in *C. trachomatis* known as CT610 has been shown to participate in this unusual route to produce folate. Interestingly, CT610 is thought to remove part of itself to donate to the molecule it produces, effectively killing the enzyme after only one reaction. In this study we show that CT610 performs very unique chemistry to ultimately facilitate the production of folate to allow *C. trachomatis* to survive. This knowledge could be used in the future for the design of antibiotics specifically targeting *C. trachomatis* and thus treating the infections caused by this organism.

Acknowledgments

My completion of this thesis was only possible due to several individuals at Virginia Tech. First, I would like to thank Dr. Kylie Allen for being a supportive mentor and for pushing me during these last two years. I would like to thank the members of my committee, Dr. Pablo Sobrado and Dr. Justin A. Lemkul for their support and helpful suggestions. I thank Andrew Pedraza for helping me with this project and my fellow graduate students in the Allen lab for their help. Finally, I thank my support system in Blacksburg who have been there for me through everything.

Contents

Abstract ii

General audience abstract iv

Acknowledgements v

Contents vi

List of Figures ix

List of Tables xi

1 Introduction 1

1.1 Chlamydia and folate biosynthesis 1

1.1.1 *Chlamydiae* 1

1.1.2 Folate biosynthesis 2

1.2 CT610: A Moonlighting Protein 5

1.2.1 CT610 induces host cell apoptosis 5

1.2.2 CT610 identified as a probable redox enzyme 6

1.2.3 CT610 involved in a novel *de novo* folate biosynthesis pathway 8

1.2.4 CT610 orthologs 10

1.3 Nonheme Diiron Oxygenases and Other Similar Enzymes 11

1.3.1 Methane Monooxygenase 13

1.3.2 Ribonucleotide reductase 15

1.3.3 CmlA 16

1.3.4 Human Heme Oxygenase 17

1.3.5 Mixed-valent diiron sites and MIOX 17

1.3.6 PqqC 18

1.4 Self-Sacrificing Enzymes 19

1.4.1 THI4p 19

1.4.2 THI5 21

1.4.3 LarE 22

1.4.4 BioU 22

1.5 Proposed Mechanism for CT610 23

References 25

2 Biochemical Characterization of CT610 from *Chlamydia trachomatis* 29

2.1 Abstract 29

2.2 Introduction 30

2.3 Materials and methods 32

2.3.1 Materials 32

2.3.2 Overexpression and purification of CT610 33

2.3.3 *In vitro* enzymatic assays and pABA detection by LC-MS 34

2.3.4 Hansatech oxygraph detection of CT610 oxygenase activity 35

2.3.5 Reconstitution of CT610 36

2.3.6 EPR sample preparation 36

2.3.7 EDTA experiments 37

2.3.8 $^{18}O_2$ experiments 38

2.3.9 MS experiments to identify amino acid modifications 38

2.4 Results 39

2.4.1 Overexpression and purification of CT610 39

2.4.2 CT610 WT pABA synthase and oxygenase activity 40

2.4.3 Fe/Fe reconstitution of CT610 41

2.4.4 pABA synthase and oxygenase activity of CT610 variants 42

2.4.5 Electron Paramagnetic Resonance (EPR) characterization 44

2.4.6 Other metal reconstitutions 45

2.4.7 EDTA experiments 47

2.4.8 $^{18}O_2$ experiments 48

2.4.9 MS experiments to identify potentially modified active site residues 49

2.5 Discussion 50

2.5.1 Metal cofactor 51

2.5.2 Potential self-sacrificing residues 54

2.6 Future Directions 57

References 60

List of Figures

1.1 Chlamydial infection cycle 2

1.2 The canonical *de novo* biosynthesis of tetrahydrofolate 4

1.3 A timeline of the main discoveries of CT610 7

1.4 The structure of CT610 7

1.5 Structural comparison of CT610 to several other proteins 12

1.6 Mechanism of methane oxidation by sMMO hydroxylase component 14

1.7 Proposed mechanism for THI4-p catalyzed thiamine biosynthesis in *S. cerevisiae* 21

1.8 Proposed mechanism for CT610-derived pABA biosynthesis 24

2.1 SDS Page gel showing a typical CT610 WT purification 39

2.2 Baseline pABA synthase and oxygenase activity of as-purified CT610 WT 41

2.3 pABA synthase and oxygenase activity of CT610 as-purified "non-reconstituted" protein vs Fe-reconstituted CT610 42

2.4 CT610 active site with highlighted residues potentially involved in the CT610 mechanism 43

2.5 pABA synthase activity and oxygenase activity of CT610 active site variants 44

2.6 X-band EPR spectra of Fe-reconstituted CT610 45

2.7 pABA synthase and oxygenase activity of CT610 reconstituted with other metals 46

2.8 Restoring pABA synthase activity after incubating CT610 with EDTA 47

2.9 $^{18}O_2$ incorporation into pABA by Mn-reconstituted CT610 48

2.10 SDS-PAGE gel showing 4 μg of protein from each of the four reactions sent for MS analysis 50

2.11 Sequence alignment comparing CT610 and NE1434 54

2.12 CT610-dependent pABA production proposed mechanism..... 56

List of Tables

1.1 Holes in the folate biosynthetic pathway in *C. trachomatis*.....3

Chapter 1:

Introduction

1.1 Chlamydia and Folate Biosynthesis

1.1.1 *Chlamydiae*

Chlamydiae are obligately intracellular bacterial pathogens that are known to infect a wide range of hosts and are the causing agent of the most frequently reported bacterial sexually transmitted infection (STI) in the United States[4]. There are 13 species of chlamydia: *C. trachomatis, C. pneumoniae, C. abortus, C. caviae, C. felis, C. muridarum, C. pecorum, C. psittaci, C. suis, C. avium, C. gallinacea, C. serpentis, and C. poikilothermis, C. ibidis, C. corallus, and C. sanzinia*[5]. *C. trachomatis* strictly infects humans and is the causing agent of STIs as well as trachoma, a leading cause of blindness in Asia and Africa[5, 7]. *C. pneumoniae* can infect both humans and other animals to cause extreme respiratory tract infections. Other species such as *C. abortus, C. caviae, C. felis, C. pecorum, C. psittaci,* and *C. suis* primarily infect animals resulting in huge economic losses by causing disease in livestock[5].

Chlamydiae follow a unique growth cycle as the infection develops[9]. An elementary body (EB) is an infectious, metabolically inactive form of the bacterium that facilitates survival in an extracellular environment. Once an EB invades a host cell, it differentiates into a noninfectious, metabolically active form called a reticulate body (RB). The RB will then divide rapidly while importing many of its essential nutrients from its host cell. Finally, all the RBs are converted

back to EBs which are released to the surrounding extracellular environment as a result of inducing host cell apoptosis[9] (Figure 1.1).

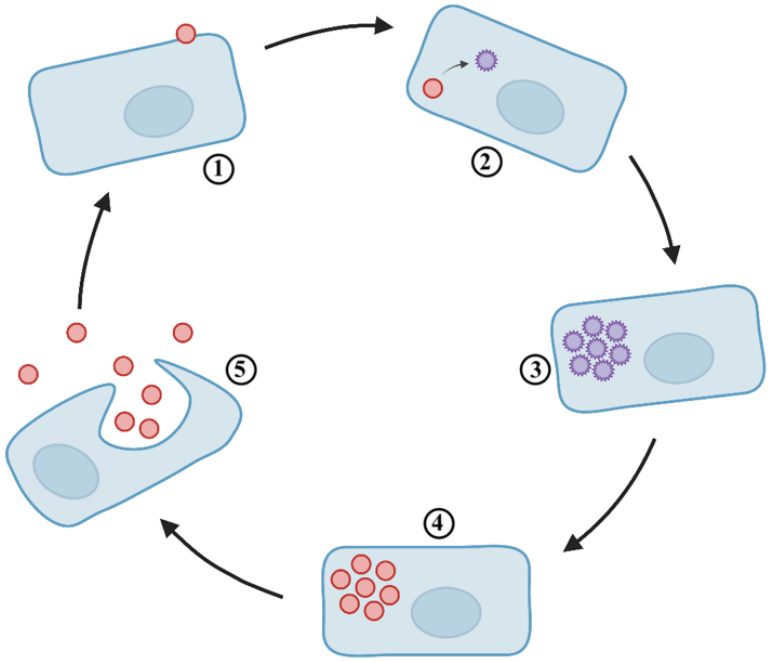

Figure 1.1 Chlamydial infection cycle. (1) EB (red) attaches and invades the host cell (blue cell). (2) EB differentiates to RB (purple) inside the host cell. (3) RB replicates inside the host cell uptaking many necessary nutrients from the host. (4) RBs redifferentiate back into EBs before (5) the new EBs are released back into the extracellular matrix after the host cell is lysed. EBs are then free to infect new host cells.

1.1.2 Folate Biosynthesis.

Tetrahydrofolate (THF) is a one-carbon carrier cofactor essential for DNA and amino acid biosynthesis and, therefore, essential to all organisms. THF is comprised of three moieties: a pteridine ring, *p*-aminobenzoate (pABA), and a variable number of glutamate residues (Figure 1.2A)[2]. Due to the essential nature of THF for cell growth and upkeep, the *de novo* biosynthesis of folate is very well-characterized. GTP is ultimately converted to the pteridine ring requiring enzymes FolEQBK, while pABA is synthesized from the precursor chorismate by PabA/B and

PabC. The pteridine ring and pABA moieties are then combined by FolP and finally, a variable number of glutamate residues are added on by FolC (Figure 1.2B)[2].

Intracellular pathogens undergo reductive evolution over time characterized by a significant loss of biosynthetic genes because the intracellular pathogens could instead uptake most of their nutrients from their host cell to save energy[7]. Interestingly, even though *C. trachomatis* is an intracellular pathogen, it has retained its ability to synthesize folate *de novo* as well as possibly being capable of transporting folate from outside the cell[2, 9]. Several genes encoding enzymes required for the canonical folate biosynthesis pathway in *C. trachomatis* are missing, including *pab*A/B and *pab*C, which are normally required for pABA biosynthesis from chorismate (Table 1.1)[6, 9]. Previous investigation showed that RibA (GTP cyclohydrolase II) and TrpF (*N*'-5'-phosphoribosylanthranilate isomerase) functionally replace FolE and FolQ in *C. trachomatis* to produce the pteridine ring moiety and an archaeal γ-glutamyl ligase is used to functionally replace FolC in the addition of glutamate residues to the folate molecule[6]. It was also found that a single gene in *C. trachomatis*, CT610, functionally replaces the canonical pABA biosynthesis genes[6]. Originally, CT610 was named Chlamydia protein associating with death domains (CADD) after it was discovered to play a role in inducing host cell apoptosis during chlamydial infection[3].

C. trachomatis	Pteridine Ring	*p*ABA	Glutamate Residues
Missing	*folE, folQ*	*pabA/B, pabC*	*folC*
Replacement	*ribA, trpF*	*ct*610	γ-glutamyl ligase

Table 1.1 Holes in the folate biosynthetic pathway in *C. trachomatis* showing the missing genes present in the canonical folate *de novo* biosynthesis pathway as well as *C. trachomatis* genes that have been shown to functionally replace these missing genes.

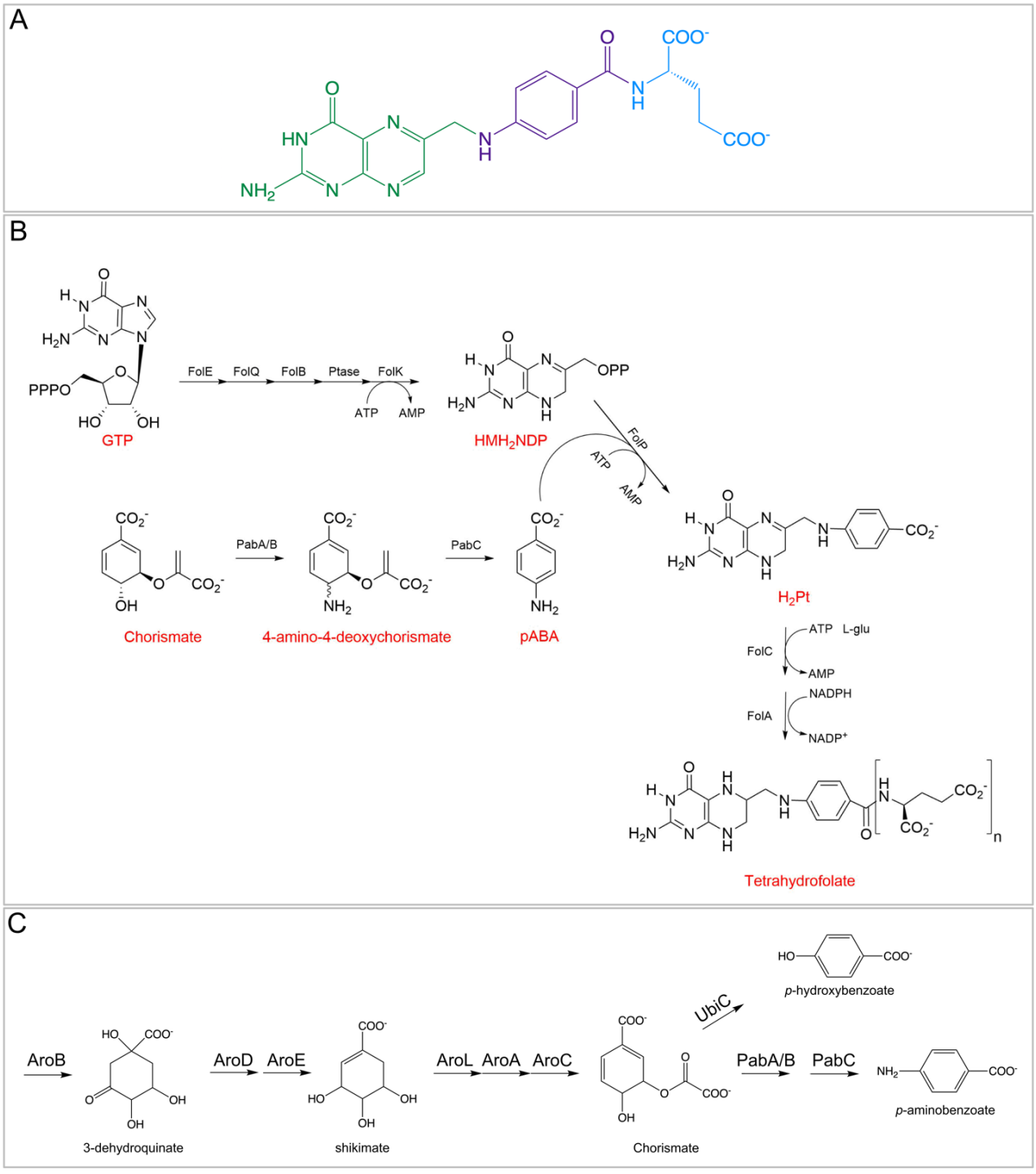

Figure 1.2 Tetrahydrofolate (THF) and its canonical *de novo* biosynthesis. (A) Structure of THF with the three moieties highlighted in green (pteridine ring), purple (pABA), and light blue (glutamate residues). (B) Canonical *de novo* biosynthesis of folate. First, GTP is converted to 6-hydroxymethyl-7,8-dihydropterin diphosphate (HMH_2NDP) by FolEQBK and chorismate is converted to pABA by PabA/B and PabC. These two resulting molecules are combined by FolP and a variable number of glutamate residues are added by FolC. (C) Condensed shikimate pathway based on Figure 1 from Macias-Orihuela et al. 2020[8].

1.2 CT610: A Moonlighting Protein

1.2.1 CT610 induces host cell apoptosis.

As part of the Chlamydial infection cycle, the bacterium eventually induces host cell apoptosis (Figure 1.1). Apoptosis can be induced via one of two pathways: the intrinsic/mitochondrial pathway or the extrinsic/death receptor pathway[12]. The intrinsic pathway uses non-receptor-mediated signaling from outside the cell that induces apoptosis by targeting the mitochondrial membrane[13]. Stimuli like hormones and cytokines actively suppress apoptosis via the intrinsic pathway and an absence of these stimuli allow for the production of intracellular signals that then promote apoptosis[13]. The extrinsic pathway involves a transmembrane "death" receptor mediated process. These death receptors are part of the Tumor Necrosis Factor (TNF) receptor family that is composed of cysteine-rich extracellular domains, and a cytoplasmic domain specifically called the "death domain" that is responsible for translating the extracellular death signal into further intracellular signaling pathways[13]. First, a trimeric TNF ligand will bind to the extracellular receptor causing the receptor to oligomerize while activating the death domain on the inside of the cell allowing it to bind to pro-apoptotic proteins such as FAS-associated death domain protein (FADD). This complex produces a death-inducing signal which ultimately leads to the activation of proteolytic caspase proteins that cleave various intracellular proteins ultimately inducing cell apoptosis[13, 14].

It was initially hypothesized that there are Chlamydiae proteins like FADD that are involved in the induction of host cell apoptosis characterized with chlamydial infection[3]. Bioinformatic analysis of the *C. trachomatis* genome revealed several proteins with a large amino acid sequence homology to death domains of mammalian TNF receptor family proteins.

One of these proteins, Chlamydia protein associating with death domains (CADD, encoded by CT610 in *C. trachomatis*), was shown to induce apoptosis in a variety of mammalian cell lines. It was shown that CT610 interacts with the death domains of TNF family receptors TNFR1, Fas, DR4, and DR5 to induce apoptosis[3].

CT610 has a 18% sequence identity with PqqC, which participates in part of the six-step biosynthesis of bacterial coenzyme PQQ (pyrroloquinoline quinone)[15]. However, *C. trachomatis* lacks homologs for the other enzymes required for the biosynthesis of PQQ[1]. The expression of PqqC from *Klebsiella pneumonia* also failed to induce host cell apoptosis like CT610, suggesting these two proteins have similar structures but likely different functions[3].

1.2.2 CT610 identified as a probable redox enzyme.

Shortly after CT610 was shown to play a role in host cell apoptosis (Figure 1.3), the crystal structure was solved. Since CT610 was characterized as playing a role in host cell apoptosis, it was expected it would have a structure like that of other death-domain associating proteins such as FADD. However, surprisingly, the structure of CT610 did not show the expected structure of a protein that associates with a death domain and instead resembled nonheme diiron oxygenases[1]. The crystal structure revealed a homodimer with two seven-helix bundles with each monomer containing a diiron cofactor (Figure 1.4A). The homodimer is formed by association of helices H2 and H3A (residues 59-85) and is primarily formed by hydrophobic interactions but also includes some polar interactions and salt bridges[1]. The proteins with the greatest sequence identity to CT610 were found to be PqqC (18%), human heme oxygenase (11%), R2 subunit of ribonucleotide reductase (R2 RNR) (12%), and the α-subunit of soluble methane monooxygenase (sMMO) (9%)[16].

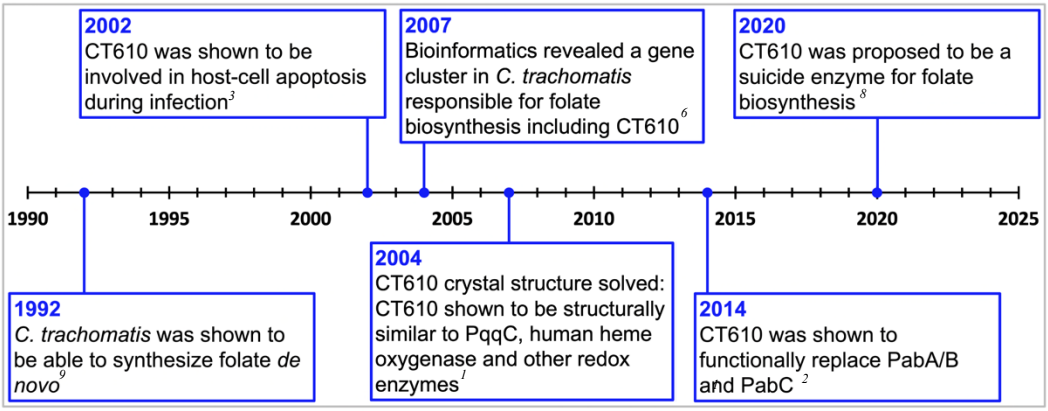

Figure 1.3 A timeline of the main discoveries surrounding CT610 (Previously labeled as CADD).

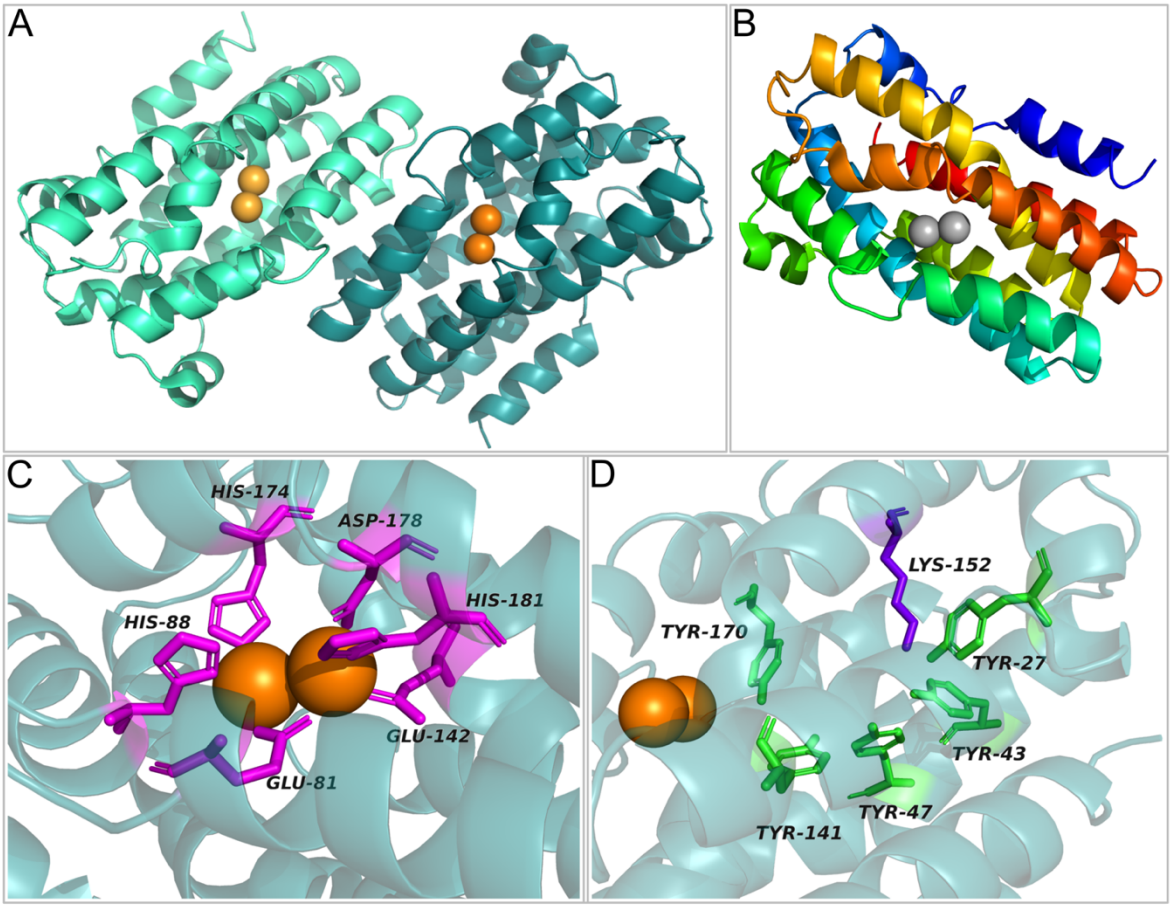

Figure 1.4 Structure of CT610 PDB 1RCW. (A) Dimer configuration of CT610 with the diiron cofactors of each monomer shown in orange. (B) CT610 monomer colored rainbow where blue represents the N-terminus while red shows the C-terminus. The diiron cofactor is shown in gray. (C) CT610 active site with the diiron cofactor shown in orange, and its coordinating residues shown in magenta. (D) CT610 active site with the diiron cofactor shown in orange, and the tyrosine and lysine residues potentially involved in CT610-catalyzed pABA production are shown in green and purple respectively.

The active site is a narrow pocket formed by the seven helices where the diiron cofactor is coordinated by 6 residues: Glu-81, His-88, Glu-142, His-174, Asp-178 and His-181 (Figure 1.4C)[1]. All six metal coordinating residues are conserved among CT610 orthologs in other chlamydia species. Interestingly, the apoptotic ability of CT610 significantly decreased when the metal coordinating residues were subjected to site-directed mutagenesis[1]. The diiron site is found in the center of the protein directly adjacent to the active site cavity. The crystal structure showed that there was a possibly a reactive oxygen species bound to the diiron site[1]. The active site of CT610 is structurally like that of R2 RNR with the main difference being that CT610 does not contain any conserved residues analogous to the catalytic residues in R2 RNR suggesting these enzymes might not function via the same catalytic mechanism[1]. Most of the metal-coordinating residues for sMMO and CT610 are conserved, and they both have a tunnel-like internal cavity adjacent to the diiron active site which serves as the site of catalysis in sMMO[1]. This suggested that CT610 could have a similar function to sMMO. The active sites of PqqC and CT610 are the least conserved out of the three, which suggests a similarity in overall structure but not function between these two enzymes[1].

1.2.3 CT610 involved in a novel *de novo* folate biosynthesis pathway.

Because CT610 is not structurally like death domain associating proteins and instead appears to structurally resemble redox proteins, it is likely that this enzyme has multiple moonlighting functions where the protein can act as a toxin released by chlamydial cells to induce host cell apoptosis and potentially use its redox function in the production of pABA for *de novo* folate biosynthesis.

Previously, it was shown that *C. trachomatis* can synthesize folate *de novo*[9]. Additionally, CT610 can complement an *E. coli* Δ*pabABC* mutant that cannot otherwise synthesize pABA, and therefore folate, resulting in the inability for these cells to grow without a source of pABA[2]. This suggests that CT610 provides this source of pABA allowing for the Δ*pabABC* cells to grow without exogenous pABA. Chorismate is the precursor for pABA in the canonical pathway for folate biosynthesis (Figure 1.2C), however, CT610 was still able to complement *E. coli* Δ*aroA* mutants that are unable to synthesize chorismate, suggesting that this metabolite was not the substrate for CT610 (Figure 1.2C)[2]. It was then thought that a different compound found in the shikimate pathway could possibly instead be the precursor for CT610-dependent pABA synthesis. Two other compounds upstream of chorismate in the shikimate pathway, shikimate and 3-dehydroquinate, were investigated to see if they could possibly be the precursor to CT610-dependent pABA synthesis. CT610 was also able to complement *E. coli ΔaroD ΔpabA* and *E. coli ΔaroB ΔpabA,* which are auxotrophic for 3-dehydroquinate and shikimate, respectively (Figure 1.2C), suggesting that the precursor to CT610-synthesized pABA is likely not part of the shikimate pathway. Finally, an *E. coli ΔubiC ΔpabA* mutant was used to investigate if ubiquinone or its precursor *p*-hydroxybenzoate was the substrate for CT610 (Figure 1.2C). However, CT610 was also able to complement this strain, suggesting that the CT610 substrate is not ubiquinone or any intermediate from the shikimate pathway[2].

Aromatic amino acids and *p*-hydroxybenzoate (pHB) had to be supplemented in the minimal media of most of the previously mentioned genetic experiments and therefore it was hypothesized that the precursor for this unusual pABA-producing enzyme could possibly be L-tyrosine or p-hydroxybenzoate (pHB)[8]. Thus, *E. coli* Δ*pabA* cells expressing CT610 were fed isotopically labeled versions of these potential precursors and the isotopic composition of the

resulting pABA was measured. In the pHB experiments, about 15% of pABA was shown to be labeled, suggesting that pHB could possibly serve as a precursor or an intermediate to pABA in CT610-dependent pABA biosynthesis[8]. Most interestingly, it was also shown that about 40% of pABA was labeled when deuterium-labeled L-tyrosine was used (50% of the tyrosine supplied was unlabeled), providing strong evidence that L-tyrosine is a precursor to pABA when synthesized by CT610[8]. Since the crystal structure showed CT610 to most likely act as an oxygenase, *ΔpabA E. coli* cells were grown anaerobically in the presence of CT610. Cells supplemented with pABA grew in this anaerobic environment, however, the cells that depended on CT610 to synthesize pABA did not grow. This suggests that CT610 requires O_2 to function[8].

Further, *in vitro* experiments with purified CT610 showed that the enzyme produces pABA in the absence of any substrates, only requiring molecular oxygen and a reducing agent such as dithiothreitol (DTT). The addition of pHB or L-tyrosine to these reactions failed to increase the amount of pABA produced, suggesting that these are not the substrates for this enzyme. **These results are consistent with CT610 acting as a unique self-sacrificing enzyme that likely cleaves one of its active site tyrosine residues to donate to the final pABA molecule[8].**

1.2.4 CT610 orthologs.

Similarly to *C. trachomatis*, a bioinformatics study identified one gene in *Nitrosomonas europaea*, NE1434, that complemented Δ*pabABC* mutants of *E. coli* without supplementation with pABA on minimal media. The genome of *N. europaea* is also missing many of the genes that synthesize folate via the canonical biosynthesis pathway. It was also found that chorismate and all the other intermediates from the shikimate pathway were also not the precursor for NE1434 mediated pABA biosynthesis[17, 18]. There is another similar ortholog found in *Lactobacillus*

fermentum. This organism was found to not require added pABA to grow, suggesting it synthesizes this molecule *de novo. L. fermentum* however, was also missing several genes in the canonical folate biosynthesis pathway including *pabABC* [19].

It seems that there are several examples of organisms that synthesize folate *de novo* via a pathway distinct from the canonical folate biosynthesis pathway. It is possible that both *N. europaea* and *L. fermentum* synthesize pABA via a similar self-sacrificing mechanism as CT610 in *C. trachomatis*. Indeed, recent work in our laboratory has shown that NE1434 exhibits similar catalytic behavior to CT610.

1.3 Nonheme Diiron Oxygenases and Other Similar Enzymes

Nonheme diiron oxygenases use nonheme diiron active sites to catalyze a wide range of reactions from the simple oxidation of Fe^{2+} to Fe^{3+} by ferritins to the hydroxylation of C–H bonds of methane[20]. Many of these enzymes consist of 4-helix bundle motifs housing diiron sites coordinated usually by carboxylate-rich residues (Figure 1.5)[20]. The catalytic cycles for most of these enzymes begin when the ferrous diiron active site reacts with O_2 generating a highly reactive intermediate at the site of the cofactor that can result in the cleavage of strong C–H or O–H bonds[20]. No matter the mechanism, most of these enzymes start with the diiron cofactor in its reduced and active Fe^{II}/Fe^{II} form and ends with a Fe^{III}/Fe^{III} cluster that can be reduced for further turnovers[20, 21].

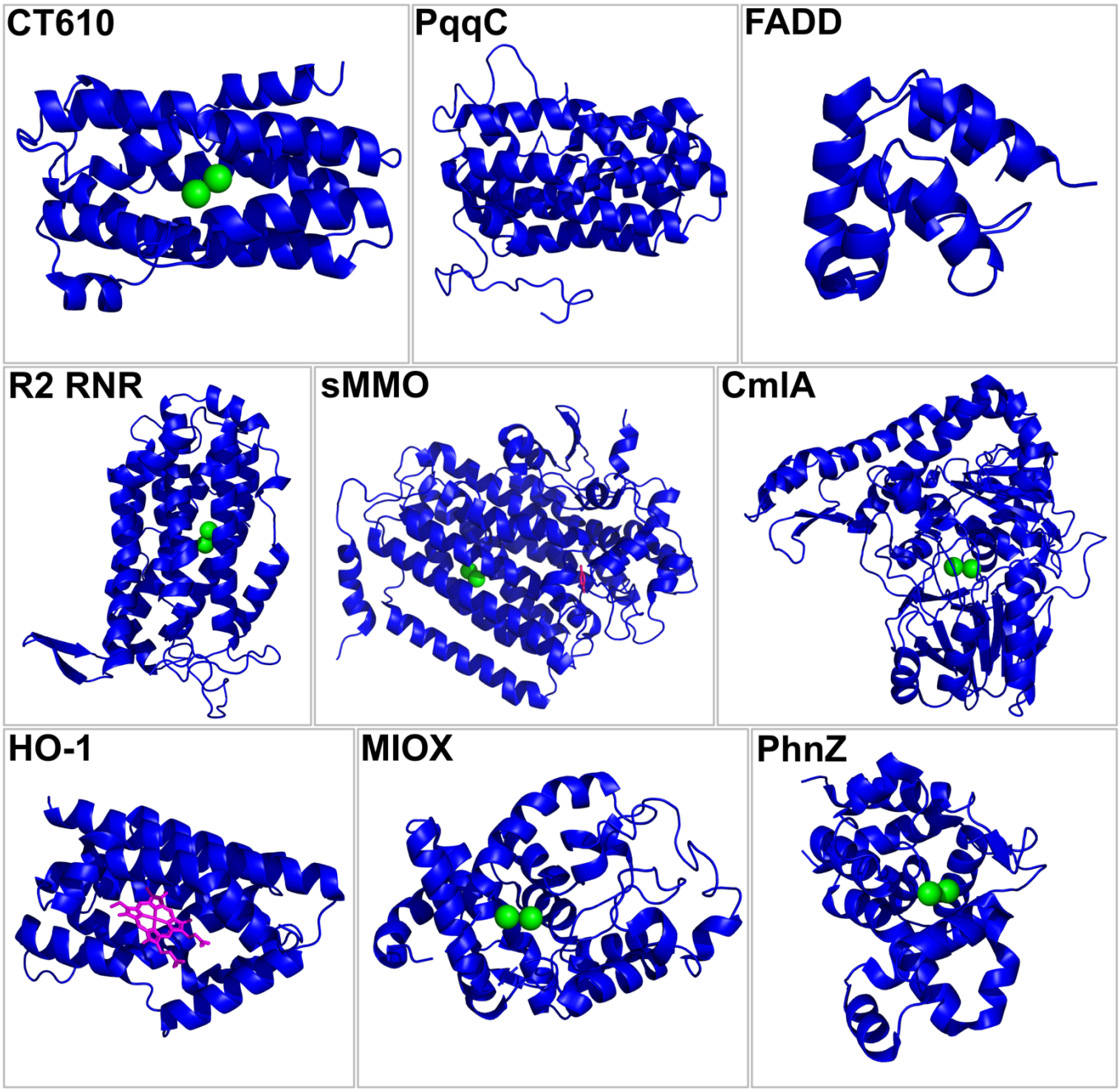

Figure 1.5 Structural comparison of CT610 to several other enzymes where any diiron active sites present are highlighted in green and any other miscellaneous cofactors are shown in magenta.

1.3.1 Methane Monooxygenase

Methane monooxygenases (MMOs) use O_2 to oxidize methane to methanol. There are two MMOs that are distinct from each other. The first is soluble MMO (sMMO) that uses a diiron active site for catalysis and the second is a membrane-bound MMO that uses a copper cofactor (pMMO) for catalysis[16]. sMMO requires three subunits to perform at maximal catalytic activity: the hydroxylase (MMOH), the reductase (MMOR) and the regulatory protein (MMOB). MMOH is an $\alpha_2\beta_2\gamma_2$ homodimer that contains a diiron cofactor in the active site of each α subunit (Figure 1.5)[16, 22]. In the catalyzed reaction two electrons are transferred from NADH to MMOR's FAD cofactor ultimately placing the electrons in a [2Fe-2S] cluster within MMOR[16, 23].

The two electrons in the [2Fe-2S] cluster within MMOR reduce the diiron cofactor from MMOH to its diferrous form (Figure 1.6, species 1) causing a carboxylate shift at one of the metal coordinating glutamate residues, allowing for O_2 to enter the active site. Dioxygen first enters the active site (Figure 1.6, species 2) before binding to the cofactor and two intermediates are formed (Figure 1.6, species 3 and 4) as the metal cofactor transfers electrons to the bound oxygen atoms shifting the cofactor to the diferric state. The reactive methane-oxidizing form of the cofactor is then produced by O–O bond cleavage. This reactive intermediate (Figure 1.6, species 5) abstracts a hydrogen from methane, producing a diiron cluster-bound hydroxyl radical intermediate (Figure 1.6 species 6) and a methyl radical. Finally, recombination of the radicals yields methanol and a cluster Fe^{III}/ Fe^{III} intermediate (Figure 1.6 species 7). Methanol is released and the oxidized state of the diiron cluster is formed. Further reduction by MMOR reproduces the diferrous cofactor and can begin this catalytic cycle again[11, 16, 23, 24].

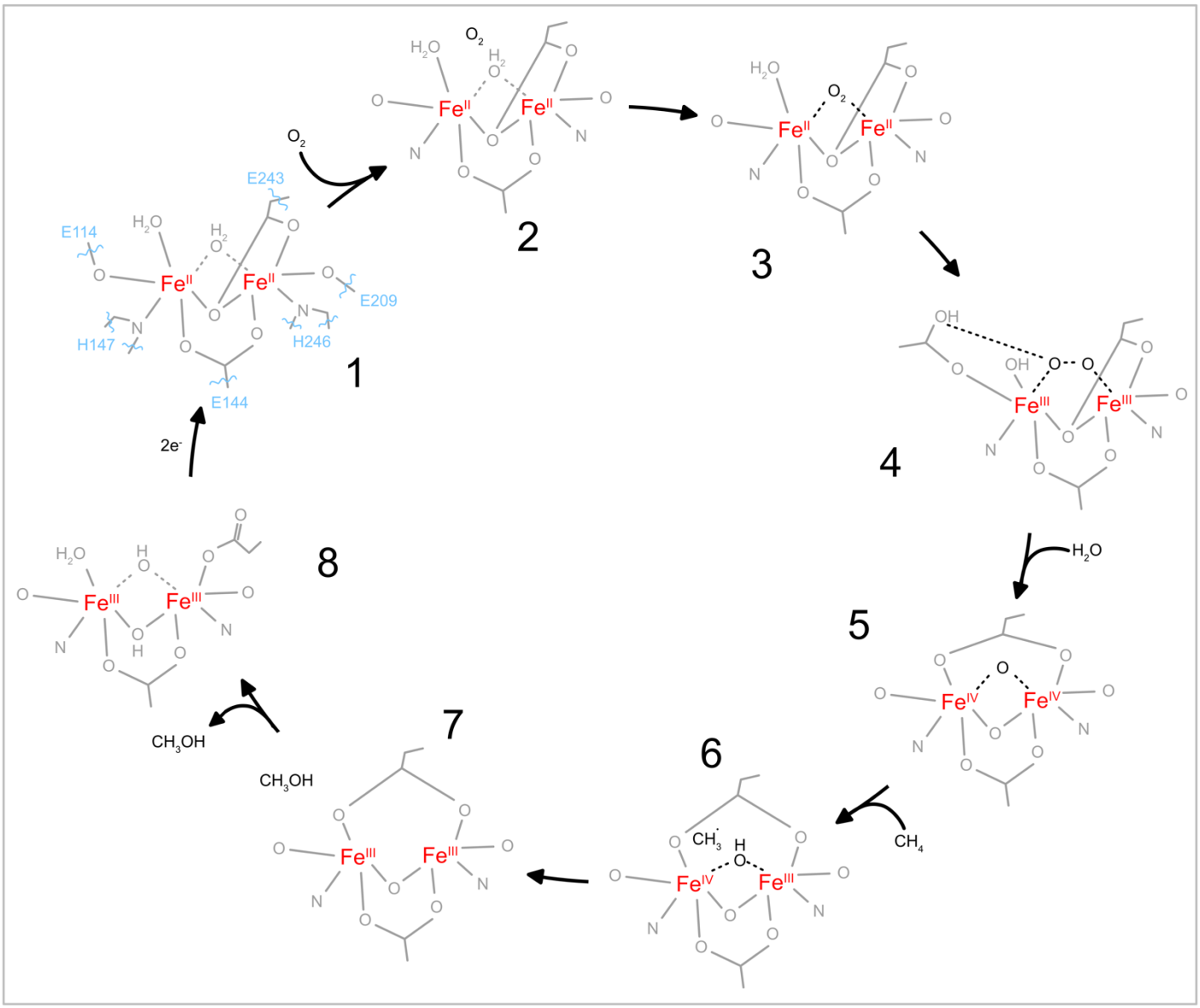

Figure 1.6 Mechanism of sMMO hydroxylase component where the diiron cofactor is shown in red, coordinating residues are shown in grey and O_2 and other key bonds are shown in black. Coordinating residues are labeled in blue in species 1. Figure based on figure 4 from Banerjee et al. 2019[11]

1.3.2 Ribonucleotide Reductase

Ribonucleotide reductases catalyze the conversion of ribonucleotides to their 2'-deoxynucelotide counterparts and thus provide the necessary precursors for DNA biosynthesis and repair[20, 25, 26]. Different RNRs are classified based on the metallo-cofactor that is used in the chemistry catalyzed by the enzyme complex[25]. No matter which cofactor a RNR uses, they all have a conserved cysteine residue in the active site that is converted into a thiyl radical that initiates the reaction[26-28]. Class I RNRs are tetrameric enzymes with two α-subunits and two β-subunits ($\alpha_2\beta_2$) where the active sites is in the binding pockets of the larger α homodimers (R1) and the smaller β homodimers (R2) each contain a diiron cofactor (Figure 1.5)[27, 28].

Since RNR is present in all organisms, the mechanism is relatively thoroughly elucidated through various methods of spectroscopy. At first, the mechanism looks very similar to that of sMMO (Figure 1.6) where two electrons reduce the diiron cofactor to its diferrous form, leading to a carboxylate shift at one of the metal coordinating glutamate residues allowing for O_2 to bind to the cofactor forming two intermediates (Figure 1.6, species 3 and 4). The reactive form of the cofactor has been shown to be different from that of sMMO. The homolytic O–O bond cleavage of species 4 (Figure 1.6) instead produces a peroxodiiron(III/IV) reactive intermediate that then oxidizes an adjacent tyrosine residue generating the tyrosyl radical needed for RNR function[29]. This tyrosyl radical is then transferred to a conserved cysteine residue in the R1 active site by a long-range radical transfer pathway between the subunits[27-30]. To initiate the reaction, a ribonucleotide then binds to the already reduced R1 and the thiyl radical abstracts the 3'-hydrogen atom from the ribose ring ultimately transferring the radical to the substrate. The radical on the substrate makes the molecule more reactive towards acid-base catalysis and the 2'-OH group is protonated by the conserved cysteine residue in R1[26]. Two cysteine residues transfer a hydrogen

atom to the substrate intermediate as they are oxidized to a disulfide anionic radical. This disulfide bridge is reduced by flavoprotein thioredoxin reductase (NADPH-dependent) so that more turnovers can than occur[26, 29, 31, 32].

1.3.3 CmlA

The enzyme CmlA is part of the pathway for the biosynthesis of chloramphenicol and catalyzes the *β*-hydroxylation of a *L*-*p*-aminophenylalanine (*L*-PAPA) moiety on its nonribosomal peptide synthetase substrate CmlP–L-PAPA[20, 21]. CmlA is a monooxygenase that inserts an oxygen atom into the β-C–H bond on CmlP–*L*-PAPA. This product then continues in the biosynthetic pathway ultimately producing chloramphenicol[21]. Interestingly, the structure of CmlA does not show the 4-helix bundle protein fold that most diiron monooxygenases are known to have. Instead, the active site of this enzyme shows a metallo-β-lactamase fold[21, 33, 34]. The crystal structure shows that CmlA is a homodimer in solution and confirmed the presence of a diiron cluster ligated by the C-terminal domain (Figure 1.5)[21, 35].

The exact molecular mechanism of CmlA is not known, but various spectroscopic and structural studies have revealed enough information for the following mechanistic proposal: As the CmlA:CmlP–L-PAPA complex forms, an Fe-coordinating glutamate carboxylate shift, similar to that in sMMO and R2 RNR, occurs slightly moving the coordinating residue into a position where it can bind with the diiron cofactor simultaneously shifting the active site allowing for O_2 to access the reduced diiron cofactor[21]. This was suggested because it was seen in the crystal structure of CmlA that there was an acetate ion bound to one of the Fe in the active site instead of the expected coordinating glutamate residues, which was shown to be slightly too distant to bind to the cofactor[21]. Although the mechanism is not completely resolved, it is likely that the O–O

bond of the O_2 molecule breaks before the C–H bond breaks forming a high-valent iron-oxo intermediate like species 5 (Figure 1.6) that is able to perform this chemistry. However, the diiron active site and catalytic mechanisms of CmlA and sMMO significantly differ suggesting that perhaps a different reactive intermediate is used[21].

1.3.4. Human Heme Oxygenase.

Human Heme Oxygenase (HO) catalyzes the oxygenation of heme to iron, biliverdin and carbon monoxide requiring NADPH, O_2, and cytochrome P450 reductase[36]. There are two isozymes of HO found in humans: HO-1 is a 288-residue protein that is implicated and/or involved in oxidative stress, ischemia, hypoxia and several other diseased states. Once the heme binds to the active site in HO, it acts both as a substrate and as a cofactor in its own degradation reaction[36, 37]. Once the enzyme forms a heme-protein complex, an electron provided by NADPH-cytochrome P450 reductase reduces the ferric heme to the ferrous state as a molecule of O_2 binds to the pocket. Then, another electron further reduces this intermediate to produce a reactive hydroxylating species hydroperoxyl-ferri-HO. This reaction mechanism ultimately ends up with iron, biliverdin and carbon monoxide being released as products[36, 38].

1.3.5 Mixed valent diiron sites (MIOX).

The mechanism for nonheme diiron oxygenases is very versatile allowing for a wide range of important reactions to proceed. However, the limitation of this conserved mechanism is that only two electrons at most can be extracted from the substrate since the electrons are typically donated to the diiron cofactor ultimately by NADPH[20, 39]. The enzyme *myo*-inositol oxygenase (MIOX) catalyzes the ring opening glycol cleavage of *myo*-inositol (MI) to D-glucuronate (DG).

This enzyme was unexpectedly discovered to contain a non-heme diiron cluster even though this reaction is a four-electron oxidation and structurally belongs to the HD-protein superfamily making it the first enzyme of this group to contain a diiron cofactor[39]. It was determined that only one molecule of DG was produced per O_2 ruling out a mechanism in which two sequential two-electron oxidations by two equivalents of O_2 using a mechanism similar to sMMO and R2 RNR[39, 40].

Once the structure of MIOX was solved, it was determined that the diiron cofactor is buried within a four-helix bundle like most nonheme diiron oxygenases however, the arrangement of the helices and the fact that it has a fifth helix makes the overall structure unique (Figure 1.5)[39, 41]. It was discovered using Mössbauer and electron paramagnetic resonance (EPR) spectroscopies that the active form of MIOX is when the diiron cofactor is in its mixed-valent (II/III) state[39, 41-43]. It was shown that the Fe^{III}/Fe^{III} form of the cofactor is reduced producing the Fe^{II}/Fe^{III} mixed valent cofactor. The substrate then binds to the Fe(III) of the cofactor before oxygen binds to the Fe(II) of the cofactor forming a (superoxo)diiron(III/III) reactive intermediate. It is then proposed that a hydrogen atom is abstracted from C1 of the bound substrate forming a C1 radical, which ultimately leads to the ring opening of MI. Further characterization of the following intermediates would need to occur for the rest of the ring-opening mechanism[39, 41-43].

1.3.6 PqqC

Pyrroloquinoline quinone (PQQ) is a common redox cofactor for bacterial dehydrogenases[15]. The enzyme that catalyzes the final step of PQQ biosynthesis is PqqC and, although this enzyme is not part of the nonheme diiron oxygenase family of enzymes, CT610 has the most similar sequence identity to PqqC. PqqC is a 251-residue protein that forms a homodimer

in solution. PqqC folds into a seven-helix bundle with six outer helices surrounding a mostly hydrophobic inner helix (Figure 1.5)[15]. It was shown that upon binding of the substrate PqqC undergoes a large conformational change that allows for several key residues to form hydrogen bonds with the substrate.

PqqC catalyzes an eight-electron oxidation through four oxidations using the following proposed mechanism that does not require any cofactors [44]: In the first step, the substrate, 3a-(2-amino-2-carboxyethyl)-4,5-dioxo-4,5,6,7,8,9-hexahydroquinoline-7,9-dicarboxylic acid (AHQQ), undergoes a two-electron oxidative ring closure using O_2. This resulting intermediate then undergoes three more two-electron oxidations two of which use O_2 and one uses H_2O_2 that is produced in the preceding step. These last three steps all have characterized intermediates, but the order of these reactions is unknown[15, 44].

1.4 Self-Sacrificing Enzymes

We propose that CT610 catalyzes its reaction via a self-sacrificing mechanism where an active site tyrosine residue is putatively cleaved off to serve as the substrate for pABA synthesis and a lysine residue serves as the amino group donor. Although self-sacrificing mechanisms seem energetically wasteful, there are few examples similar mechanisms characterized.

1.4.1 THI4p

Thiamine pyrophosphate (TPP) is an essential cofactor in all organisms that consists of two precursors, one of which being a thiazole ring. The mechanistic details for how prokaryotes

synthesize this thiamine thiazole are well characterized and require five enzymes to do so[10, 45]. In eukaryotes, however, there is only one encoded protein that synthesizes the thiamine thiazole, THI4p (from *Saccharomyces cerevisiae*)[10]. The source of the thiamine thiazole ring sulfur remained elusive leaving the mechanism of this enzyme initially unclear. However, it was later discovered that the recombinantly expressed THI4p WT exhibited a mass that was around 34 Da lower that the calculated mass of the enzyme, while several active site mutants did not show any activity and exhibited the expected mass of the enzyme, suggesting this loss in mass was in some way related to the catalytic activity[10]. It was then shown that the sulfur source for the synthesis of the thiamine thiazole was derived from the Cys205 residue within the enzyme itself. *In vitro* reactivation of this enzyme proved unsuccessful and a 1:(1.1±0.2) stoichiometry was seen between THI4p and the resulting thiamine produced. This evidence suggested that the cysteine residue was cleaved off leaving the -34 Da mass difference in a single turnover reaction mechanism[10].

THI4p does not contain a diiron cofactor but it was shown that the residue cleaving reaction does not occur without the addition of Fe^{II}. In the proposed mechanism of this reaction, Fe^{II} is coordinated by the thiol and carbonyl of the sulfide donating cysteine residue. As the intermediate binds to the thiol of the cysteine residue, a hydrogen abstraction by a general base causes the sulfide transfer to the product of this reaction, cleaving the sulfide from the cysteine residue (Figure 1.7).

Since a cell uses a large amount of energy to synthesize proteins, it is confusing why an enzyme would be made to turnover only once in its lifetime. However, just like CT610, THI4p seems to moonlight in other functions. It was shown that strains of *S. cerevisiae* that had disrupted thi4 genes showed an increase sensitivity to treatment with DNA damaging ultraviolet radiation[46].

It was shown that THI4p is involved in both thiamine thiazole biosynthesis as well as DNA damage tolerance perhaps explaining why this enzyme might use this peculiar mechanism of catalysis.

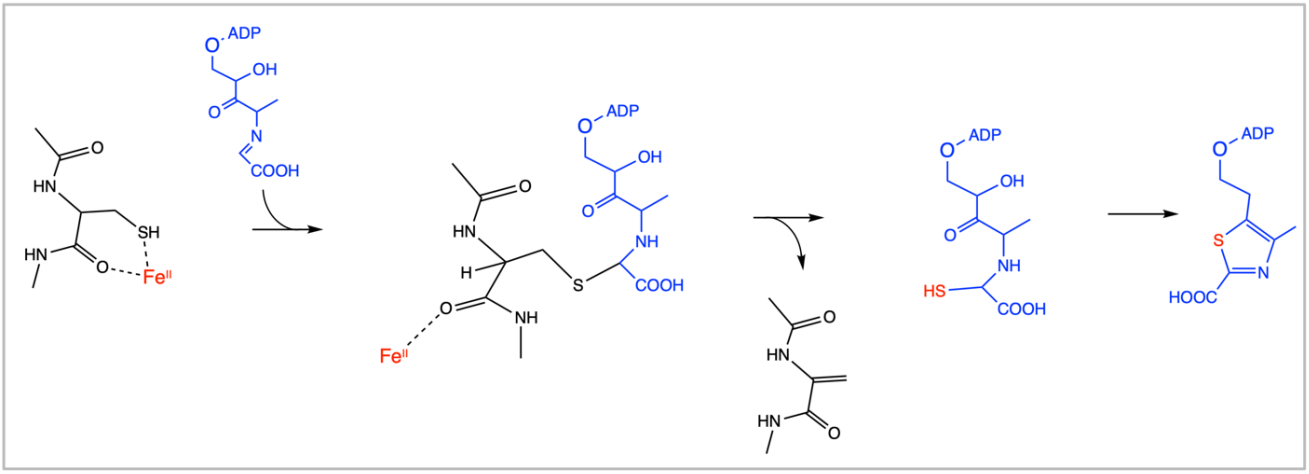

Figure 1.7 Proposed Thi4p mechanism based on figure 4e from Chatterjee et al. 2011[10]

1.4.2 THI5

THI5 synthesizes 4-amino-2-methyl-5-hydrohymethylpyrimidine phosphate (HMP-P) as part of thiamin pyrophosphate biosynthesis in *S. cerevisiae*. THI5 generates HMP-P from histidine and pyridoxal phosphate (PLP). Like CT610, THI5 did not require the addition of histidine (the substrate) to stimulate the catalytic activity of the enzyme. Analysis through mass spectrometry reveled incorporation of ^{15}N into the HMP-P molecule when the enzyme was expressed in minimal media containing ^{15}N-ammonium chloride suggesting that a his residue from THI5 itself was possibly the source of the incorporated nitrogens[47]. The proposed mechanism of this enzyme describes a azadiene part of an intermediate undergoing a Diels-Alder reaction with the CN bond from the donating histidine residue[47].

1.4.3 LarE

Lactate Racemase (Lar) converts D- and L-lactic acid providing both stereoisomers to the microorganism. The enzyme LarA harbors a covalently bound Ni pincer complex which is the first of its kind identified in the natural world and many Ni pincer complexes tend to be very reactive[48]. Synthesis of this novel cofactor requires enzymes LarB, LarC and LarE. It was shown that LarE was responsible for the sulfur insertion into the LarA cofactor, however, the source of this sulfur was unknown. Analysis through mass spectrometry revealed that the mass of LarE after its catalyzed reaction was 34 Da less than that of the initial enzyme. Furthermore, it was shown that a cysteine residue was replaced with dehydroalanine suggesting that LarE donates sulfur to the LarA Ni pincer cofactor by donating cys176 in a single turnover self-sacrificing mechanism[48].

1.4.4 BioU

The biosynthesis of biotin is well characterized and involves the conversion of pimeloyl intermediates to biotin catalyzed by enzymes BioF, BioA, BioD and BioB. It was found that *Cyanobacterium synechocystis* is missing a gene homolog for BioA but had still been shown to synthesize biotin itself. It was then discovered that a novel dehydrogenase BioU functionally replaces BioA catalyzing three different reactions[49]. In one of these reactions, the ε-amino group of Lys124 is carboxylated before the cleavage and release of this residue to act as the amino donor for the product of this reaction 7,8-diaminononate (DAN) that ultimately becomes biotin through the rest of the biosynthetic pathway[49]. Interestingly, we propose a similar scenario for CT610, where an active site lysine residue is utilized as the amino donor.

1.5 Proposed Mechanism for CT610

Since CT610 resembles a nonheme diiron oxygenase, we proposed that it would function similarly to sMMOH and R2 RNR. It is unknown what reduces CT610 *in vivo* but it is possible the cofactor is reduced by a reductase protein like in sMMOH or the electrons might be donated more directly.

An overview of our proposed mechanism is shown in Figure 1.8. Two electrons are transferred to the diiron cofactor reducing them to the diferrous state, which presumably causes a carboxylate shift at one of the metal coordinating residues, allowing for O_2 to enter the active site and binds to the cofactor forming intermediates similar to sMMO (Figure 1.6, species 3 and 4) as the metal cofactor transfers electrons to the bound oxygen atoms shifting the cofactor to the diferric state. The reactive bis-μ-oxo-Fe^{IV} intermediate is produced by O–O bond cleavage. This reactive intermediate abstracts a hydrogen from the *β*-carbon of the tyrosine residue, producing a diiron cluster-bound hydroxyl radical intermediate like Figure 1.6 species 6 and a radical on the *β*-carbon of the tyrosine. Finally, recombination of the radicals would allow hydroxylation of the *β*-carbon, which activates the molecule for base catalyzed cleavage of the Cα-Cβ bond, releasing the tyrosine residue from the backbone and yielding *p*-hydroxybenzaldehyde and a Fe^{III}/ Fe^{III} intermediate (Figure 1.6 species 7). The cofactor is reduced to the diferrous state again allowing for another radical hydroxylation reaction producing *p*-hydroxybenzoate (pHB). This molecule is then aminated, dehydrated and rearranged to produce pABA (Figure 1.8)[8].

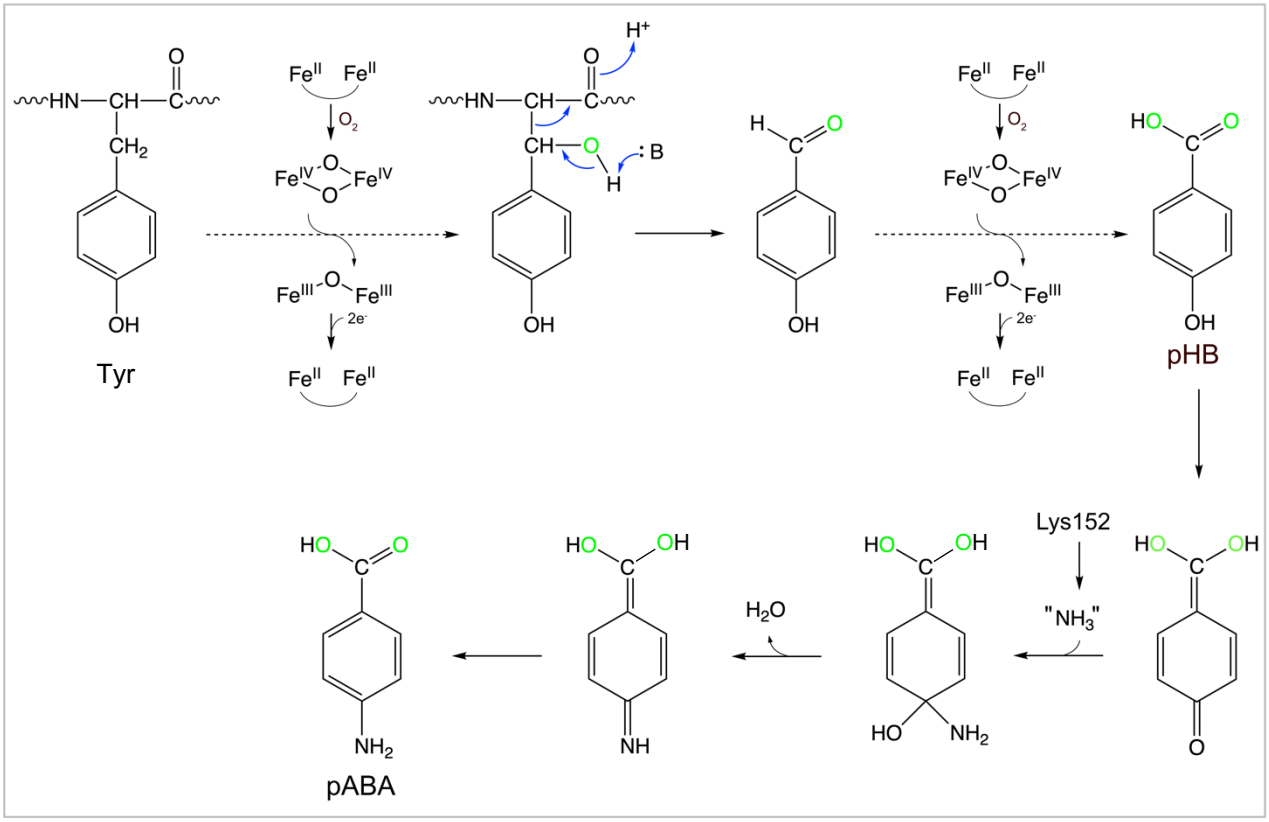

Figure 1.8 Proposed mechanism for CT610-derived pABA biosynthesis where CT610-incorporated oxygens are shown in green.

References:

[1] Schwarzenbacher, R., Stenner-Liewen, F., Liewen, H., Robinson, H., Yuan, H., Bossy-Wetzel, E., Reed, J. C., and Liddington, R. C. (2004) Structure of the Chlamydia protein CADD reveals a redox enzyme that modulates host cell apoptosis, *J Biol Chem 279*, 29320-29324.

[2] Adams, N. E., Thiaville, J. J., Proestos, J., Juárez-Vázquez, A. L., McCoy, A. J., Barona-Gómez, F., Iwata-Reuyl, D., de Crécy-Lagard, V., and Maurelli, A. T. (2014) Promiscuous and adaptable enzymes fill "holes" in the tetrahydrofolate pathway in Chlamydia species, *mBio 5*, e01378-01314.

[3] Stenner-Liewen, F., Liewen, H., Zapata, J. M., Pawlowski, K., Godzik, A., and Reed, J. C. (2002) CADD, a Chlamydia protein that interacts with death receptors, *J Biol Chem 277*, 9633-9636.

[4] (2021) Chlamydia Statistics, https://www.cdc.gov/std/chlamydia/stats.htm.

[5] Cheong, H. C., Lee, C. Y. Q., Cheok, Y. Y., Tan, G. M. Y., Looi, C. Y., and Wong, W. F. (2019) Chlamydiaceae: Diseases in Primary Hosts and Zoonosis, *Microorganisms 7*.

[6] de Crécy-Lagard, V., El Yacoubi, B., de la Garza, R. D., Noiriel, A., and Hanson, A. D. (2007) Comparative genomics of bacterial and plant folate synthesis and salvage: predictions and validations, *BMC Genomics 8*, 245.

[7] Zomorodipour, A., and Andersson, S. G. (1999) Obligate intracellular parasites: Rickettsia prowazekii and Chlamydia trachomatis, *FEBS Lett 452*, 11-15.

[8] Macias-Orihuela, Y., Cast, T., Crawford, I., Brandecker Kevin, J., Thiaville Jennifer, J., Murzin Alexey, G., de Crécy-Lagard, V., White Robert, H., Allen Kylie, D., and Metcalf William, W. (2020) An Unusual Route for p-Aminobenzoate Biosynthesis in Chlamydia trachomatis Involves a Probable Self-Sacrificing Diiron Oxygenase, *Journal of Bacteriology 202*, e00319-00320.

[9] Fan, H., Brunham, R. C., and McClarty, G. (1992) Acquisition and synthesis of folates by obligate intracellular bacteria of the genus Chlamydia, *J Clin Invest 90*, 1803-1811.

[10] Chatterjee, A., Abeydeera, N. D., Bale, S., Pai, P. J., Dorrestein, P. C., Russell, D. H., Ealick, S. E., and Begley, T. P. (2011) Saccharomyces cerevisiae THI4p is a suicide thiamine thiazole synthase, *Nature 478*, 542-U146.

[11] Banerjee, R., Jones, J. C., and Lipscomb, J. D. (2019) Soluble Methane Monooxygenase, *Annu Rev Biochem 88*, 409-431.

[12] Kun, D., Xiang-lin, C., Ming, Z., and Qi, L. (2013) Chlamydia inhibit host cell apoptosis by inducing Bag-1 via the MAPK/ERK survival pathway, *Apoptosis 18*, 1083-1092.

[13] Elmore, S. (2007) Apoptosis: a review of programmed cell death, *Toxicol Pathol 35*, 495-516.

[14] Yanumula, A., and Cusick, J. K. (2022) Biochemistry, Extrinsic Pathway of Apoptosis, In *StatPearls*, StatPearls Publishing

[15] Magnusson, O. T., Toyama, H., Saeki, M., Rojas, A., Reed, J. C., Liddington, R. C., Klinman, J. P., and Schwarzenbacher, R. (2004) Quinone biogenesis: Structure and mechanism of PqqC, the final catalyst in the production of pyrroloquinoline quinone, *P Natl Acad Sci USA 101*, 7913-7918.

[16] Ross, M. O., and Rosenzweig, A. C. (2017) A tale of two methane monooxygenases, *J Biol Inorg Chem 22*, 307-319.

[17] Satoh, Y., Kuratsu, M., Kobayashi, D., and Dairi, T. (2014) New gene responsible for para-aminobenzoate biosynthesis, *J Biosci Bioeng 117*, 178-183.
[18] Chain, P., Lamerdin, J., Larimer, F., Regala, W., Lao, V., Land, M., Hauser, L., Hooper, A., Klotz, M., Norton, J., Sayavedra-Soto, L., Arciero, D., Hommes, N., Whittaker, M., and Arp, D. (2003) Complete Genome Sequence of the Ammonia-Oxidizing Bacterium and Obligate Chemolithoautotroph Nitrosomonas europaea, *Journal of Bacteriology 185*, 2759-2773.
[19] Kuratsu, M., Hamano, Y., and Dairi, T. (2010) Analysis of the Lactobacillus Metabolic Pathway, *Applied and Environmental Microbiology 76*, 7299-7301.
[20] Jasniewski, A. J., and Que, L., Jr. (2018) Dioxygen Activation by Nonheme Diiron Enzymes: Diverse Dioxygen Adducts, High-Valent Intermediates, and Related Model Complexes, *Chem Rev 118*, 2554-2592.
[21] Komor, A. J., Jasniewski, A. J., Que, L., and Lipscomb, J. D. (2018) Diiron monooxygenases in natural product biosynthesis, *Nat Prod Rep 35*, 646-659.
[22] Rosenzweig, A. C., Frederick, C. A., Lippard, S. J., and Nordlund, P. (1993) Crystal structure of a bacterial non-haem iron hydroxylase that catalyses the biological oxidation of methane, *Nature 366*, 537-543.
[23] Lund, J., Woodland, M. P., and Dalton, H. (1985) Electron transfer reactions in the soluble methane monooxygenase of Methylococcus capsulatus (Bath), *Eur J Biochem 147*, 297-305.
[24] Banerjee, R., Proshlyakov, Y., Lipscomb, J. D., and Proshlyakov, D. A. (2015) Structure of the key species in the enzymatic oxidation of methane to methanol, *Nature 518*, 431-434.
[25] Minnihan, E. C., Nocera, D. G., and Stubbe, J. (2013) Reversible, long-range radical transfer in E. coli class Ia ribonucleotide reductase, *Acc Chem Res 46*, 2524-2535.
[26] Kolberg, M., Strand, K. R., Graff, P., and Andersson, K. K. (2004) Structure, function, and mechanism of ribonucleotide reductases, *Biochim Biophys Acta 1699*, 1-34.
[27] Eklund, H., Uhlin, U., Farnegardh, M., Logan, D. T., and Nordlund, P. (2001) Structure and function of the radical enzyme ribonucleotide reductase, *Prog Biophys Mol Biol 77*, 177-268.
[28] Stubbe, J., and van Der Donk, W. A. (1998) Protein Radicals in Enzyme Catalysis. [Chem. Rev. 1998, 98, 705minus sign762, *Chem Rev 98*, 2661-2662.
[29] Baldwin, J., Krebs, C., Saleh, L., Stelling, M., Huynh, B. H., Bollinger, J. M., Jr., and Riggs-Gelasco, P. (2003) Structural characterization of the peroxodiiron(III) intermediate generated during oxygen activation by the W48A/D84E variant of ribonucleotide reductase protein R2 from Escherichia coli, *Biochemistry 42*, 13269-13279.
[30] Krebs, C., Chen, S. X., Baldwin, J., Ley, B. A., Patel, U., Edmondson, D. E., Huynh, B. H., and Bollinger, J. M. (2000) Mechanism of rapid electron transfer during oxygen activation in the R2 subunit of Escherichia coli ribonucleotide reductase. 2. Evidence for and consequences of blocked electron transfer in the W48F variant, *J Am Chem Soc 122*, 12207-12219.
[31] Persson, A. L., Eriksson, M., Katterle, B., Potsch, S., Sahlin, M., and Sjoberg, B. M. (1997) A new mechanism-based radical intermediate in a mutant R1 protein affecting the catalytically essential Glu441 in Escherichia coli ribonucleotide reductase, *J Biol Chem 272*, 31533-31541.

[32] Persson, A. L., Sahlin, M., and Sjoberg, B. M. (1998) Cysteinyl and substrate radical formation in active site mutant E441Q of Escherichia coli class I ribonucleotide reductase, *J Biol Chem 273*, 31016-31020.
[33] Makris, T. M., Chakrabarti, M., Munck, E., and Lipscomb, J. D. (2010) A family of diiron monooxygenases catalyzing amino acid beta-hydroxylation in antibiotic biosynthesis, *Proc Natl Acad Sci U S A 107*, 15391-15396.
[34] Silaghi-Dumitrescu, R., Ng, K. Y., Viswanathan, R., and Kurtz, D. M., Jr. (2005) A flavo-diiron protein from Desulfovibrio vulgaris with oxidase and nitric oxide reductase activities. Evidence for an in vivo nitric oxide scavenging function, *Biochemistry 44*, 3572-3579.
[35] Makris, T. M., Knoot, C. J., Wilmot, C. M., and Lipscomb, J. D. (2013) Structure of a dinuclear iron cluster-containing beta-hydroxylase active in antibiotic biosynthesis, *Biochemistry 52*, 6662-6671.
[36] Schuller, D. J., Wilks, A., Ortiz de Montellano, P. R., and Poulos, T. L. (1999) Crystal structure of human heme oxygenase-1, *Nat Struct Biol 6*, 860-867.
[37] Ryter, S. W., Alam, J., and Choi, A. M. (2006) Heme oxygenase-1/carbon monoxide: from basic science to therapeutic applications, *Physiol Rev 86*, 583-650.
[38] Davydov, R., Kofman, V., Fujii, H., Yoshida, T., Ikeda-Saito, M., and Hoffman, B. M. (2002) Catalytic mechanism of heme oxygenase through EPR and ENDOR of cryoreduced oxy-heme oxygenase and its Asp 140 mutants, *J Am Chem Soc 124*, 1798-1808.
[39] Bollinger, J. M., Jr., Diao, Y., Matthews, M. L., Xing, G., and Krebs, C. (2009) myo-Inositol oxygenase: a radical new pathway for O(2) and C-H activation at a nonheme diiron cluster, *Dalton Trans*, 905-914.
[40] Charalampous, F. C., and Lyras, C. (1957) Biochemical studies on inositol. IV. Conversion of inositol to glucuronic acid by rat kidney extracts, *J Biol Chem 228*, 1-13.
[41] Snyder, R. A., Bell, C. B., 3rd, Diao, Y., Krebs, C., Bollinger, J. M., Jr., and Solomon, E. I. (2013) Circular dichroism, magnetic circular dichroism, and variable temperature variable field magnetic circular dichroism studies of biferrous and mixed-valent myo-inositol oxygenase: insights into substrate activation of O2 reactivity, *J Am Chem Soc 135*, 15851-15863.
[42] Xing, G., Barr, E. W., Diao, Y., Hoffart, L. M., Prabhu, K. S., Arner, R. J., Reddy, C. C., Krebs, C., and Bollinger, J. M., Jr. (2006) Oxygen activation by a mixed-valent, diiron(II/III) cluster in the glycol cleavage reaction catalyzed by myo-inositol oxygenase, *Biochemistry 45*, 5402-5412.
[43] Xing, G., Hoffart, L. M., Diao, Y., Prabhu, K. S., Arner, R. J., Reddy, C. C., Krebs, C., and Bollinger, J. M., Jr. (2006) A coupled dinuclear iron cluster that is perturbed by substrate binding in myo-inositol oxygenase, *Biochemistry 45*, 5393-5401.
[44] Bonnot, F., Iavarone, A. T., and Klinman, J. P. (2013) Multistep, eight-electron oxidation catalyzed by the cofactorless oxidase, PqqC: identification of chemical intermediates and their dependence on molecular oxygen, *Biochemistry 52*, 4667-4675.
[45] Jurgenson, C. T., Begley, T. P., and Ealick, S. E. (2009) The structural and biochemical foundations of thiamin biosynthesis, *Annu Rev Biochem 78*, 569-603.
[46] Machado, C. R., Praekelt, U. M., de Oliveira, R. C., Barbosa, A. C., Byrne, K. L., Meacock, P. A., and Menck, C. F. (1997) Dual role for the yeast THI4 gene in thiamine biosynthesis and DNA damage tolerance, *J Mol Biol 273*, 114-121.

[47] Lai, R. Y., Huang, S., Fenwick, M. K., Hazra, A., Zhang, Y., Rajashankar, K., Philmus, B., Kinsland, C., Sanders, J. M., Ealick, S. E., and Begley, T. P. (2012) Thiamin pyrimidine biosynthesis in Candida albicans : a remarkable reaction between histidine and pyridoxal phosphate, *J Am Chem Soc 134*, 9157-9159.
[48] Desguin, B., Soumillion, P., Hols, P., and Hausinger, R. P. (2016) Nickel-pincer cofactor biosynthesis involves LarB-catalyzed pyridinium carboxylation and LarE-dependent sacrificial sulfur insertion, *Proc Natl Acad Sci U S A 113*, 5598-5603.
[49] Sakaki, K., Ohishi, K., Shimizu, T., Kobayashi, I., Mori, N., Matsuda, K., Tomita, T., Watanabe, H., Tanaka, K., Kuzuyama, T., and Nishiyama, M. (2020) A suicide enzyme catalyzes multiple reactions for biotin biosynthesis in cyanobacteria, *Nat Chem Biol 16*, 415-422.

Chapter 2:

Biochemical Characterization of CT610 from *Chlamydia trachomatis*

2.1 Abstract

Folate cofactors consist of a pteridine ring, *p*-aminobenzoate (pABA), and a variable number of glutamate residues. *Chlamydia trachomatis* synthesizes folate *de novo*; however, several genes encoding enzymes required for the canonical folate biosynthesis pathway are missing, including *pabA/B* and *pabC*, which are normally required for pABA biosynthesis from chorismate. Previous genetic studies have found that a single gene in *C. trachomatis*, CT610, functionally replaces the canonical pABA biosynthesis genes. It was revealed that CT610 produces pABA without any added substrates only requiring a reducing agent and molecular oxygen. Thus, CT610 is proposed to be a self-sacrificing enzyme that uses one of its active site tyrosine residues as a precursor to pABA. Here, we discuss our progress towards understanding CT610-catalyzed pABA synthesis. Upon investigation of the pABA production and oxygenase activities of several active site tyrosine to phenylalanine variants, we found that Y27 and/or Y43 are the most likely precursors to the resulting pABA molecule. Further, activity was nearly completely abolished with a K152R variant, suggesting that this conserved lysine may be the required amino group donor. We also developed an *in vitro* Fe(II) reconstitution procedure, where the reconstituted enzyme exhibited a drastic increase in oxygenase activity but,

surprisingly, a significant decrease in pABA synthase activity. Interestingly, a significant increase in pABA synthase activity was observed when the enzyme was reconstituted with manganese as opposed to iron, suggesting that the diiron active site of this enzyme might not be directly involved in CT610-dependent production of pABA and instead Mn may be the actual cofactor. Finally, we show that two ^{18}O atoms from molecular oxygen are incorporated into the pABA molecule when synthesized by Mn-reconstituted CT610, providing further evidence for the oxygenase activity of CT610 and supporting our proposed mechanism that involves two monooxygenase reactions.

2.2 Introduction

Folate is a cofactor required for many essential processes including DNA and amino acid biosynthesis. The active cofactor tetrahydrofolate (THF) is made up of three parts: a pteridine ring, *p*-aminobenzoate (pABA), and a variable number of glutamate residues (Figure 1.2A). THF is synthesized by most plants and some bacteria, and the *de novo* biosynthesis of this cofactor has been thoroughly characterized[1]. The pteridine ring is synthesized using GTP as a substrate catalyzed by the FolEQBK enzymes[1]. pABA is synthesized using chorismate as a precursor catalyzed by PabA/B (ADC synthase) and PabC (ADC lyase). The pteridine ring and pABA are combined by FolP, glutamylated by FolC and fully reduced producing THF (Figure 1.2A)[2].

Chlamydiae are obligately intracellular bacterial pathogens that are known to infect a wide range of hosts and are the causing agent of the most frequently reported bacterial sexually transmitted infection (STI) in the United States[3]. There are 13 species of *Chlamydiae* - the most common one known to infect humans is *Chlamydia trachomatis,* which strictly infects humans

and is the causing agent of STIs as well as trachoma, a leading cause of blindness in Asia and Africa[4, 5]. Even though *C. trachomatis* is an intracellular pathogen, it has retained its ability to synthesize folate *de novo* as well as possibly being capable of transporting folate from outside the cell[2, 6]. However, several genes encoding enzymes required for the canonical folate biosynthesis pathway in *C. trachomatis* are missing, including *pab*A/B and *pab*C, which are normally required for pABA biosynthesis from chorismate (Table 1.1)[6, 7]. Previous investigation showed that RibA (GTP cyclohydrolase II) and TrpF (*N*'-5'-phosphoribosylanthranilate isomerase) functionally replace FolE and FolQ in *C. trachomatis* to produce the pteridine ring moiety and archaeal γ-glutamyl ligase is used to functionally replace FolC in the addition of glutamate residues to the folate molecule[7]. It was also found that a single gene in *C. trachomatis*, CT610, functionally replaces the canonical pABA biosynthesis genes[7].

CT610 was first discovered to play a role in inducing host cell apoptosis during chlamydial infection and was therefore originally named Chlamydia protein associating with death domains (CADD)[8]. When the crystal structure was solved however, it did not show the expected structure of a protein that associates with a death domain and instead resembled nonheme diiron oxygenases[9]. CT610 was found to be similar in sequence to PqqC (18%), human heme oxygenase (11%), R2 subunit of ribonucleotide reductase (R2 RNR) (12%), and the α-subunit of soluble methane monooxygenase (sMMO) (9%)[9]. Taken together, it is likely that CT610 moonlights both as a toxin released by chlamydial cells inducing host cell apoptosis as well as playing a key role in novel *de novo* folate biosynthesis in *C. trachomatis*.

CT610 was shown to be able to complement *E. coli* ΔaroA mutants that cannot synthesize chorismate showing that chorismate is not the substrate for CT610-catalyzed pABA (Figure 1.2C)[2]. Further complementation studies showed that 2-dehydroquinate and shikimate, upstream intermediates in the shikimate pathway were also not the substrates[2]. It was shown that CT610 incorporates isotopically labeled tyrosine into the synthesized pABA molecule however, *in vitro* experiments with purified CT610 showed that the enzyme produces pABA in the absence of any substrates. In these assays it was shown that CT610 only requires molecular oxygen and a reducing agent such as dithiothreitol (DTT) to produce pABA[10]. Further, The addition of pHB or L-tyrosine to these reactions failed to increase the amount of pABA produced, suggesting that these are not substrates for this enzyme[10]. Together, these results are consistent with CT610 acting as a unique self-sacrificing enzyme that likely cleaves one of its active site tyrosine residues to donate to the final pABA molecule[10]. Here, we report our recent progress towards understanding the mechanism of CT610-catalyzed pABA production.

2.3 Materials and Methods

2.3.1 Materials

Reducing agents – Dithiothreitol (DTT) was acquired from GoldBio, sodium dithionite was from EMPLURA, methyl viologen and ascorbic acid were from ACRŌS Organics, NADH and NADPH were from Research Products International (RPI), and FAD and Tris(2-carboxyethyl)phosphine (TCEP) were from Millipore-Sigma. Metals – Ferrous ammonium sulfate was acquired from Sigma Aldrich and copper (II) sulfate anhydrous, zinc sulfate

heptahydrate and manganese(II) sulfate monohydrate were from Alfa Aesar. Other – Ethylenediaminetetraacetic acid (EDTA) disodium salt and Oxygen $-^{18}O_2$ were from Millipore-Sigma, and primers for mutagenesis were from Integrated DNA technologies (IDT). All other reagents were from Genesee Scientific unless otherwise specified.

2.3.2 Overexpression and purification of CT610

The *ct*610 gene in pET19b was originally obtained from Anthony Maurelli (University of Florida). This construct was adjusted previously to use the proteomics-predicted start codon instead of the genomics-predicted start codon and the resulting construct (pET19b_CT610) was used for all further CT610 overexpression and purifications[10].

For overexpression of CT610 with an N-terminal 10X-His tag, the pET19b_CT610 plasmid was transformed into *E. coli* BL21 and a single colony from a LB/Amp plate was used to inoculate 30 mL of LB broth supplemented with 100 μg/mL ampicillin, which was then incubated at 37°C with shaking at 200 rpm overnight. An aliquot (15 mL) of this culture was used to inoculate 2 flasks with 1.5 L of LB broth supplemented with 100 μg/mL ampicillin and was incubated at 37°C with shaking at 200 rpm. When the optical density at 600 nm (OD_{600}) reached ~0.7, the expression of CT610 was induced by the addition of 0.5 mM isopropyl-β-D-thiogalactopyranoside (IPTG). The cells were cultured for 4 hours at 37°C, harvested by centrifugation, and stored at –20°C until the pellet was needed for purification.

A routine purification was performed from 3 L of culture resulting in a cell pellet of ~12 g. The pellet was resuspended in 30 mL 50 mM sodium phosphate, 300 mM NaCl, and 20 mM imidazole (pH 7.4) (buffer A: 20 mM imidazole). The cells were then sonicated on ice and the insoluble cell debris was removed by centrifugation at 15,000 rpm for 45 mins. The cell lysate

was loaded into a gravity flow column (1 by 5 cm, ~2 mL of resin) of Ni-nitrilotriacetic acid (Ni-NTA) metal affinity resin (Prometheus), equilibrated with 20 mL buffer A. The column was then washed with 10 mL of buffer A followed by 10 mL of buffer A: 100 mM imidazole. CT610 was then eluted from the column with buffer A: 250 mM imidazole, collecting 10 1-mL fractions followed by 2 1-mL fractions eluted with buffer A: 500 mM imidazole.

After concentrating all 12 fractions to 2.5 mL using an Amicon centrifuge concentrator (10-kDa cutoff, 15 mL; EMD Millipore), CT610 was exchanged into 20 mM Hepes (pH 7.5) using a PD-10 desalting column (GE Healthcare). The final purified protein in 3.5 mL had an average concentration of ~700 μM. All 3.5 mL of protein was flash frozen in ~1 mL aliquots using liquid nitrogen and stored at –80°C. Protein concentrations were determined by the Bradford method with bovine serum albumin as a standard.

2.3.3 *In vitro* enzymatic assays and pABA detection by LC-MS

Purified CT610 described above was thawed on ice. A typical pABA assay was a 500 μL reaction carried out in 20 mM Hepes (pH 7.5) and contained 164 μM (4.5 mg/mL) CT610 and 10 mM DTT. A negative control "protein only" reaction contained only 164 μM (4.5 mg/mL) CT610 in 20 mM Hepes (pH 7.5). The enzyme reactions were incubated at 37°C for 1 hour before the protein was quenched with 1.5 mL CH_3CN. The protein was removed by high-speed centrifugation, concentrated under a vacuum to 100 μL and analyzed by LC-MS.

When performing these assays with reconstituted protein (see below), the reconstituted sample was first oxygenated by gently pipetting up and down in an aerobic environment as well as using oxygenated 20 mM Hepes to dilute the protein for the reactions. DTT was then added and the reactions proceeded as described above.

For LC-MS analysis, a Waters Acquity TQD mass spectrometer with a Waters Acquity UPLC equipped with an Acquity Premier HSS T3 column (2.1 x 100 mm, 1.8 μm particle size) was used with solvent A as 0.1% formic acid in water and solvent B as 100% methanol. The LC program consisted of 3 min at 95% A followed by a 10-min linear gradient to 50% B at a flow rate of 0.35 mL/min and the injection volume was 10 μl. The MS method was a multiple reaction-monitoring method scanning three pairs: 138.1 and 120.4, 138.1 and 94.4, and 138.1 and 77.3, with a collision energy of 15V. The source temperature was 150°C, the desolvation temperature was 500°C, the desolvation gas flow was 800 L/hr, and the cone gas flow was 50 L/hr. MassLynx was used for system operation and data processing.

2.3.4 Hansatech Oxygraph detection of CT610 oxygenase activity

The concentration of oxygen in a 1 mL reaction was measured using an oxygen electrode system (Hansatech, Amesbury, MA). Purified CT610 described above was thawed on ice. The protein (200 μL, final concentration of 164 μM or higher) was added to 780 μL of 20 mM Hepes (pH 7.5) and the reaction was initiated by the addition of 20 μL of 0.5 M dithiothreitol. The decrease in oxygen concentration over time was measured as the enzyme consumed O_2. Each rate of O_2 consumption was transformed from μM/min to min^{-1} by dividing the initial rate by the concentration of CT610 in the reaction chamber to account for the amount of enzyme present in each reaction. Control reactions were performed with buffer + DTT in the absence of enzyme, as well as with protein in buffer only in the absence of DTT.

2.3.5 Reconstitution of CT610

A 2.5 mL sample containing no more than 180 μM (5.0 mg/mL) of CT610 was deoxygenated in an anaerobic chamber by gently stirring for 2 hours. Then, 2x molar excess ferrous ammonium sulfate was introduced to the sample and gently stirred in the anaerobic box for another two hours to allow for the Fe to fully incorporate into the enzyme active site. Finally, excess Fe was removed using a PD-10 desalting column (Cytiva Life Sciences) eluting the reconstituted protein with deoxygenated 20 mM Hepes (pH 7.5). This sample was capped to keep the sample anaerobic and stored at 4°C overnight or used for *in vitro* enzymatic assays immediately. Previous experiments showed no significant decrease in pABA production when the enzyme was left at 4°C overnight. The Fe-content of purified CT610 was determined using methods previously described[10, 11].

All other reconstitutions were performed in the same way as the Fe/Fe reconstitution except for the concentration and type of metal added. For mixed metal reconstitutions (ex: Mn/Fe), 0.5x molar excess Fe, and 1x molar excess of the other accompanying metal (Mn) was added to the sample and the rest of the reconstitution would proceed as described above. For other metal reconstitutions that did not contain Fe (ex: Mn/Mn), 2x molar excess of that metal was added to the sample just as with the Fe/Fe reconstitution. The various metal forms used were: $Cu(II)SO_4$, $Zn(II)SO_4$ and $Mn(II)SO_4$.

2.3.6 EPR sample preparation

CT610 was reconstituted with 2x molar excess Fe as described above. Three EPR samples (~164 μM) were prepared from one Fe-reconstitution. The first was deoxygenated with protein only, the second was Fe-reconstituted with no reducing agent present, the third was Fe-

reconstituted reduced with DTT, the fourth was Fe-reconstituted CT610 reduced with DTT and then oxygenated. The samples (300 μL) were transferred to 4 mm EPR tubes in the anaerobic chamber, frozen in cold isopentane (~77K), removed from the anaerobic chamber and stored in liquid nitrogen. Low temperature X-band EPR spectra were obtained on a Bruker ER073 EMX Spectrophotometer with a EMX High Sensitivity Probehead with a liquid helium variable temperature system (ER4112HV). The following conditions were used to record each spectrum: 9.376 GHz, 10 G modulation amplitude, 3400 G center field, 1000 G sweep width, 1 mW power, 0.3 s time constant, 10K, 5 X 1 min scans.

2.3.7 EDTA experiments

First, freshly purified CT610 was used to set up an *in vitro* pABA assay with and without DTT as a baseline of pABA production. Then, the same protein stock was used to create two 5 mL ~180 μM solutions of protein. One of these vials was gently stirred with 1 mM EDTA for one hour before removing the excess EDTA using a PD-10 desalting column. The other vial was stirred for one hour without EDTA and exchanged using a PD-10 desalting column to ensure that the stirring and exchanging process did not harm the enzymatic activity. The resulting protein was concentrated down to 2.5 mL and samples were taken from each vial for pABA assays described above to determine the effect of removing the metal(s) on the production of pABA. Then, the remaining samples were transferred into an anaerobic box and both samples were reconstituted as described above. Finally, these reconstituted protein samples (one treated with EDTA and one not) were used to set up final pABA assays to determine if reconstituting the protein could restore pABA production even after stripping out the cofactor.

2.3.8 $^{18}O_2$ experiments

Freshly purified CT610 was reconstituted as described above. The next day, the protein was further deoxygenated by gently stirring in an anaerobic chamber for one hour. Then, the deoxygenated sample was used to set up two 1.5 mL pABA assays with 164 μM CT610. These samples were reduced with 10 mM DTT in the anaerobic chamber, capped and removed from the box. The N_2 and H_2 present in the sample vials from the anaerobic chamber were removed with a vacuum and one of the vials was flushed with $^{18}O_2$ while the other vial was flushed with $^{16}O_2$ from a syringe filled with air. These reactions were incubated at 37°C in a water bath for 2 hours before the reactions were quenched with 4.5 mL acetonitrile. The protein was removed by high-speed centrifugation and concentrated under a vacuum to 100 μL for LC-MS analysis. The method was a general MS scan from 50-200 *m/z* and using other parameters described above.

2.3.9 MS experiments to identify amino acid modifications

A portion of purified CT610 was reconstituted with Mn-only and the remaining non-reconstituted CT610 protein stock was used to set up two *in vitro* pABA assays as detailed above with and without DTT added to the reactions. The Mn-reconstituted CT610 was then used to set up two *in vitro* pABA assays as detailed above with and without DTT. After incubating these reactions for 1 hour, instead of quenching with acetonitrile, 2 μg and 4μg of CT610 from each of these four reactions were loaded on an SDS-PAGE gel and sent MS analysis where the bands were excised, and the stain was removed. The protein samples were reduced with DTT and alkylated with iodoacetamide (IAA) to remove any cysteine disulfide bonds and to alkylate free sulfhydryl groups. The samples were then digested with Pierce™ Glu-C Serine Protease, MS grade from ThermoFischer Scientific. LC-MS/MS analysis was performed on the samples using

a Lumos Fusion Orbitrap (ThermoFischer Scientific) and the data was analyzed using Proteome Discover 2.5 (ThermoFischer Scientific) and Mascot 2.7 (Matrix Science).

2.4 Results

2.4.1 Overexpression and purification of CT610

CT610 containing a 10X-His-tag was overexpressed and purified from *E. coli* BL21 (Figure 2.1). A routine purification yielded a final protein concentration of 20 mg/mL (~700 μM) in 3.5 mL. On average, non-reconstituted CT610 contained ~0.02-0.05 mol Fe per mol of the enzyme, suggesting that the majority of the enzyme population is missing the diiron cofactor.

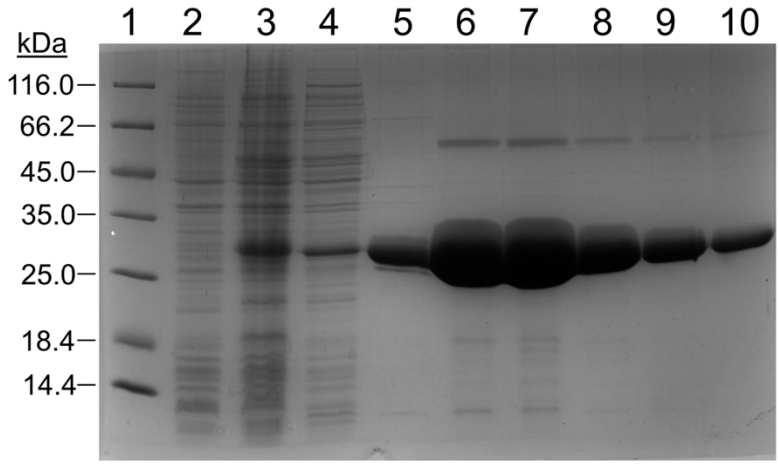

Figure 2.1 SDS-PAGE gel showing a typical CT610 WT purification. Left to right: (1) molecular weight marker (2) T0 induction study (3) TF induction study (4) wash fraction (5-10) collected purified fractions.

2.4.2 CT610 WT pABA synthase and oxygenase activity

To confirm the pABA synthase activity of CT610, reactions with the purified enzyme were carried out in the presence vs. absence of DTT[10]. An as-purified non-reconstituted CT610 produced an average of ~3 μM pABA when the enzyme is incubated with DTT versus ~1.5 μM pABA detected when incubated without a reducing agent (Figure 2.2A). The pABA present in the negative control is likely due to either pABA bound to the purified enzyme or a small amount of the enzyme being produced with an active form of the cofactor as the protein is overexpressed in *E. coli*. Several other reducing agents were tested, but it was clear that incubating the enzyme with DTT produced significantly more pABA compared to the other reducing agents (Figure 2.2B). Additionally, experiments were repeated with L-tyrosine, *p*-hydroxyphenylpyruvate, and *p*-hydroxybenzoate as potential substrates, which confirmed previously reported results that these molecules do not result in increased pABA formation by CT610 and thus are not substrates[10].

An as-purified non-reconstituted CT610 consumed oxygen at an average rate of ~0.12 min^{-1} (Figure 2.2C) when the enzyme was incubated with DTT and virtually no oxygenase activity when a reducing agent was not included in the reaction. The oxygenase activity of non-reconstituted CT610 was recorded using approximately triple the amount of enzyme as compared to all the following data. This was because adding ~164 μM of the non-reconstituted protein does not show any measurable oxygenase activity likely because most of the protein is missing the required diiron cofactor. Since the rate of oxygen consumption for all data points were converted to min^{-1} by dividing by the concentration of enzyme used for comparison between experiments, a high concentration of non-reconstituted CT610 was used to obtain a baseline of oxygen consumption for the as-purified protein.

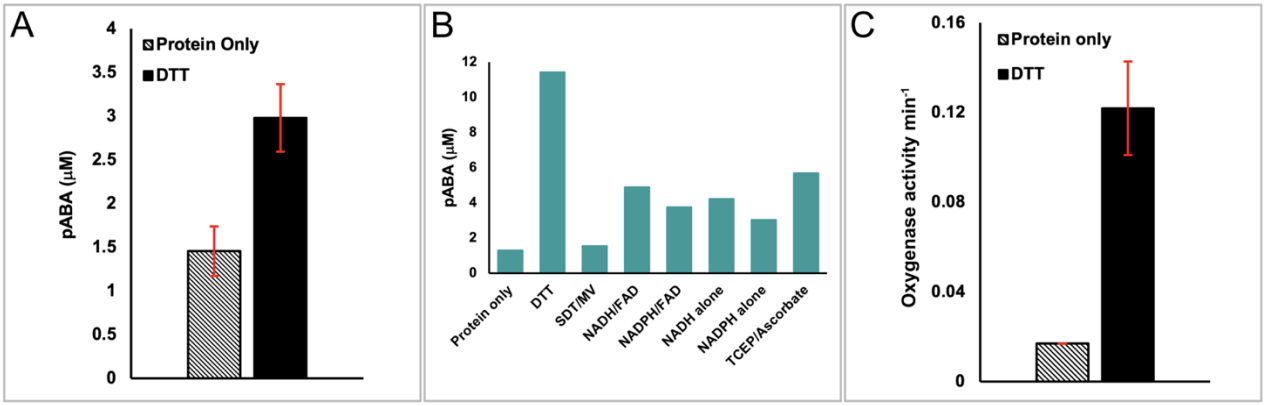

Figure 2.2 Baseline pABA synthase and oxygenase activity of as-purified CT610 WT. (A) pABA synthase activity of CT610 protein only compared to the enzyme in the presence of DTT as a reducing agent. (B) pABA production of as-purified CT610 in the presence of several reducing agents. (C) Oxygenase activity of CT610 protein only compared to the enzyme in the presence of DTT as a reducing agent.

2.4.3 Fe/Fe reconstitution of CT610

Since the crystal structure revealed that CT610 had a diiron cofactor and the as-purified enzyme only purified with ~0.05 mol Fe per mol protein, a reconstitution procedure was performed in an attempt to increase the *in vitro* enzymatic activity. When CT610 was reconstituted with Fe(II), the Fe-content of the sample increased from ~0.05 to ~1.75 mol Fe per mol protein suggesting that a significant percentage of the reconstituted CT610 monomers contain a diiron cofactor. We predicted a significant increase in pABA production from the reconstituted enzyme since the diiron cofactor was thought to play a key role in pABA production. However, the pABA production of Fe-reconstituted CT610 substantially decreased compared to the non-reconstituted enzyme (Figure 2.3A). This led us to believe that the diiron cofactor might not be the relevant cofactor for pABA synthase activity.

Contrastingly, the rate of oxygen consumption of the reconstituted protein greatly increased from ~0.12 min^{-1} to ~3.0 min^{-1} (Figure 2.3B). Clearly, reconstituting with Fe(II) drastically increased the protein's ability to consume oxygen. However, since the pABA synthase activity was significantly decreased, the oxygenase activity and pABA synthase activity were not inherently coupled. These data further led to the conclusion that the enzyme did not require the diiron cofactor for pABA production and that possibly some other metal cofactor was being used to perform this chemistry.

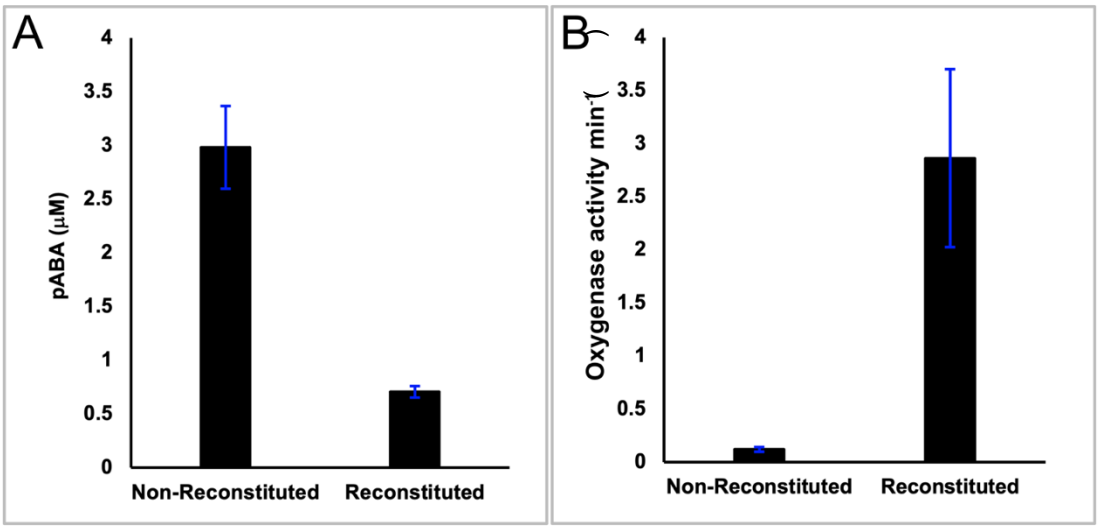

Figure 2.3 (A) pABA synthase activity of CT610 as-purified "non-reconstituted" protein vs Fe-reconstituted CT610. (B) Oxygenase activity of CT610 non-reconstituted protein vs Fe-reconstituted CT610

2.4.4 pABA synthase and oxygenase activity of CT610 variants

We previously proposed that CT610 uses a self-sacrificing mechanism to synthesize pABA, where one of the active site tyrosine residues, and potentially a conserved lysine residue, are used as substrates for pABA synthesis[10]. To attempt to narrow down the active site residues involved in catalysis, we compared the pABA synthase and oxygenase activity of six active site mutants (Y27F, Y43F, Y47F, Y141F, Y170F, and K152R) (Figure 2.4). Because the Fe-

reconstitution greatly increased the oxygenase activity of the enzyme, all oxygraph data was acquired using reconstituted variants. However, since this reconstitution significantly decreased the pABA synthase activity, all *in vitro* pABA production assays were performed with non-reconstituted variants.

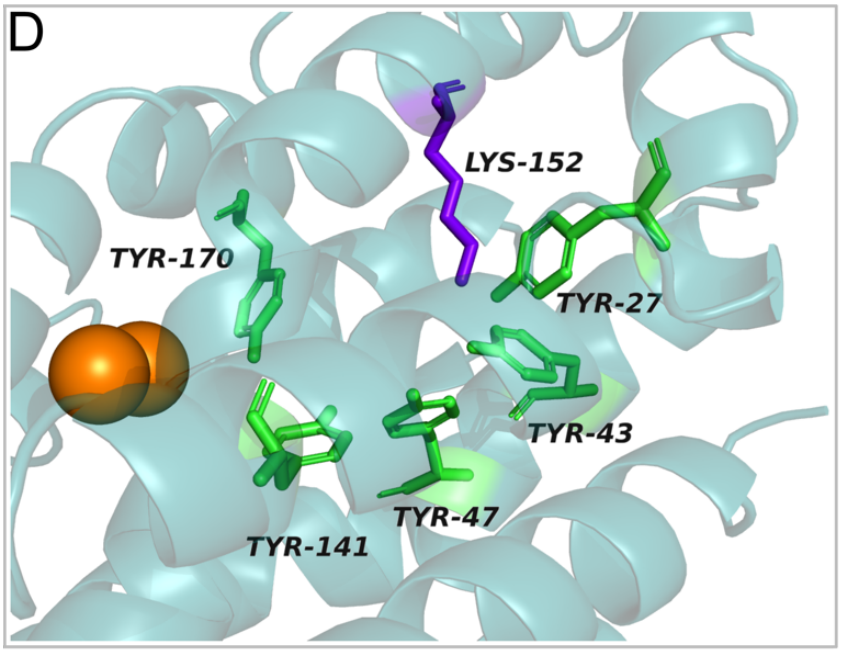

Figure 2.4 CT610 active site with the diiron cofactor shown in orange, and the tyrosine and lysine residues potentially involved in CT610-catalyzed pABA production are shown in green and purple respectively.

The amount of pABA produced by the CT610 variants compared to both reconstituted and non-reconstituted CT610 WT is shown in Figure 2.5A. None of the variants produced as much pABA as the WT; however, the Y27F and Y43F variants showed the greatest decrease in pABA production. This is consistent with the fact that these two tyrosine residues are conserved in the CT610 ortholog in *Nitrosomonas europaea* NE1434 while the Y170 and Y141 equivalent residues are replaced naturally with phenylalanine in NE1434. Y47 is also a conserved tyrosine residue in NE1434 however the Y47F variant produced significantly more pABA than the Y27F

and Y43F variants. This suggests that the cleaved tyrosine residue in CT610-catalzyed pABA production can likely be narrowed down to Y27 and/or Y43. Similarly, the activity of the K152R variant was shown to be drastically decreased (Figure 2.5A), suggesting this residue may also be involved in catalysis, possibly as the unknown amino group donor.

Interestingly, the oxygenase activity of all these variants seems to follow the opposite pattern as the pABA synthase activity, where reconstituted Y27F, Y43F, and K152R consumed the most oxygen and all had similar oxygenase activities as the reconstituted WT (Figure 2.5B). This pattern seems to show once again that the pABA synthase activity and Fe^{II}-dependent oxygenase activity of CT610 seem to be uncoupled or unrelated in some way.

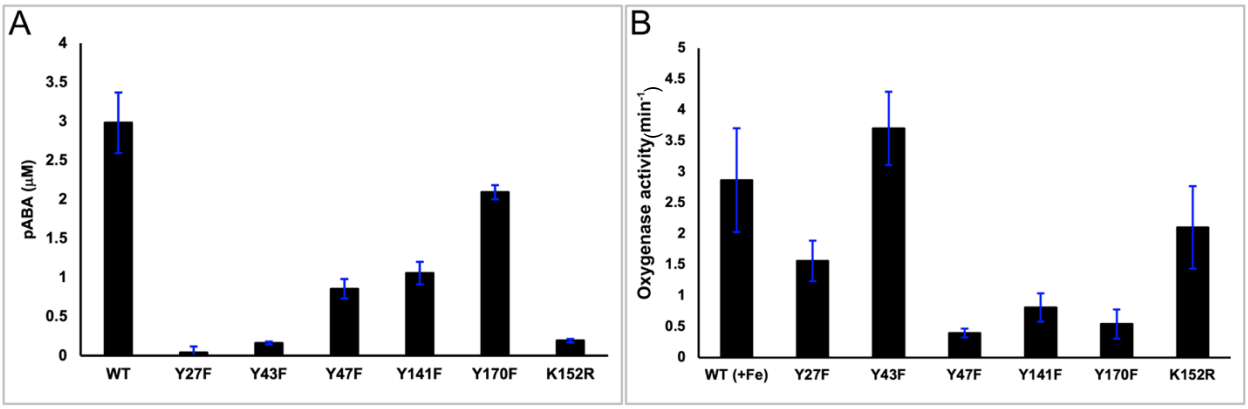

Figure 2.5 pABA synthase activity and oxygenase activity of CT610 active site variants. A) pABA synthase activity of non-reconstituted and reconstituted CT610 WT compared to reconstituted CT610 active site mutants B) Oxygenase activity of non-reconstitute

2.4.5 Electron Paramagnetic Resonance (EPR) characterization

The EPR spectra of CT610 in three different conditions are shown in Figure 2.6. The first spectrum (green) shows a baseline control of deoxygenated Fe-reconstituted CT610 without any reducing agent. When DTT was added, a very similar spectrum is observed (orange). Finally, once the reduced, Fe-reconstituted CT610 was introduced to O_2, a strong EPR signal at g~2.0

was observed, suggesting the presence of an unpaired electron. Presumably this is due to the reduced diiron cofactor reacting with the introduced O_2.

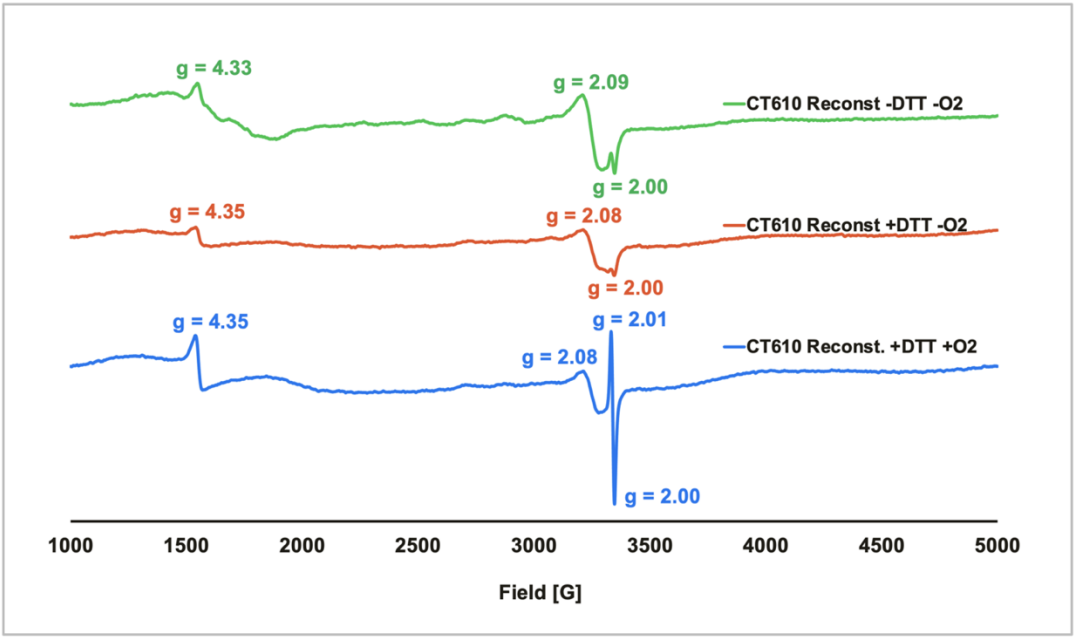

Figure 2.6 X-band EPR spectra of anaerobic reconstituted CT610 WT protein only sample vs. anaerobic reconstituted CT610 WT +DTT vs. reconstituted CT610 WT +DTT (oxygenated). Spectra were recorded at 10K.

2.4.6 Other metal reconstitutions

Since reconstitution of CT610 increased the oxygenase activity but significantly decreased the pABA synthase activity of the enzyme, we proposed that possibly a different metal could serve as a cofactor for this enzyme that was being replaced with iron during the reconstitution procedure. To test this, CT610 was reconstituted with Zn(II), Cu(II) and Mn(II) as well as Fe(II) paired with each of the other previous three metals.

Interestingly, when CT610 was reconstituted with Zn, Cu, and Mn there was a large increase in the resulting pABA synthase activity when compared to the non-reconstituted and Fe-reconstituted enzymes (Figure 2.7A). The Mn-reconstitution showed the largest increase in

pABA production followed closely by the Mn/Fe-reconstitution (Figure 2.7A). Only 1x molar excess of Mn was added in the Mn/Fe reconstitution whereas 2x molar excess Mn was added in the Mn-reconstitution. This could suggest that Mn is not replacing the Fe in the active site but instead binding elsewhere since theoretically only one Mn atom would be present per monomer of CT610 in the Mn/Fe reconstituted CT610 reactions that both resulted in very similar amounts of pABA produced.

Each of these reconstitutions were repeated and their oxygenase activities were analyzed using a Hansatech oxygraph. Interestingly, none of the other metal reconstitutions showed a significant increase in oxygenase activity like the Fe-reconstitution (Figure 2.7B). A slight increase in oxygen consumption was shown primarily in the mixed reconstitutions (like Mn/Fe) most likely due to a small increase in the amount of enzymes containing Fe in the diiron active site. Since the Fe-reconstitutions seem to be consuming O_2 at a greatly increased rate, but a there is also a decrease of the amount of pABA formed, it is likely that the Fe present in the Fe-reconstituted CT610 reactions is reacting with O_2 but not actually completing any kind of productive reaction.

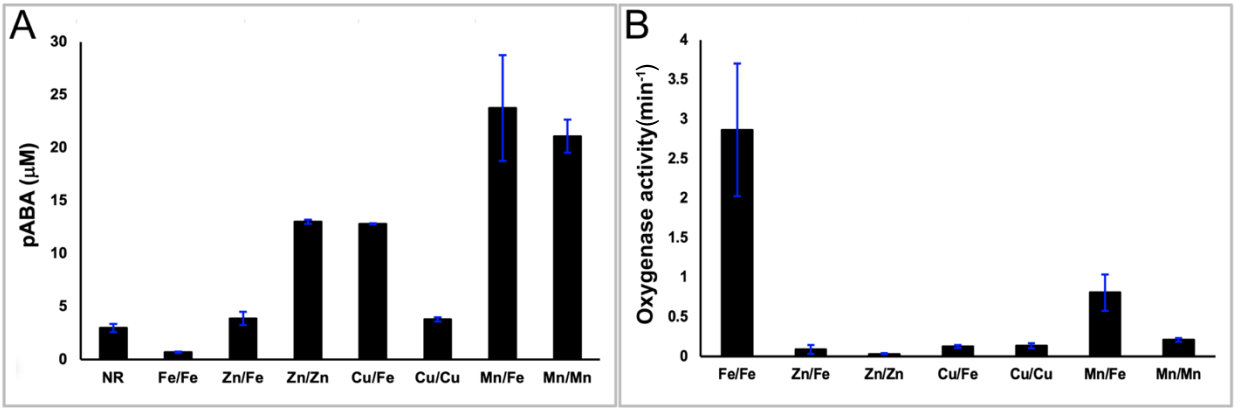

Figure 2.7 pABA synthase and oxygenase activity and pABA synthase activity of CT610 when reconstituted with iron only, zinc and iron, zinc only, copper and iron, copper only, manganese and iron and manganese only compared to the non-reconstituted enzyme.

2.4.7 EDTA experiments

To attempt to negate the apparent pABA found in the negative control (protein only) samples and to confirm the identity of the metal cofactor required for pABA synthesis, CT610 was treated with EDTA to remove any existing metals bound to the as-purified enzyme. Then, this sample of CT610 was reconstituted to restore the pABA synthase activity of the enzyme. Figure 2.8A shows this experiment with a Fe-reconstitution while Figure 2.8B shows this experiment with a Mn-reconstitution. The protein that was incubated with EDTA in both cases showed a large decrease in pABA that was produced. Once the EDTA treated protein was reconstituted (with either Fe or Mn), the pABA synthase activity was shown to be restored to that of the reconstituted protein that was not treated with EDTA. The Mn-reconstituted protein shows at least a 30-fold increase pABA synthase activity than the Fe-reconstituted protein depending on the protein prep. A small amount of pABA is still seen in the negative controls of the EDTA treated reconstituted proteins, suggesting that a fraction of the protein may purify with pABA bound.

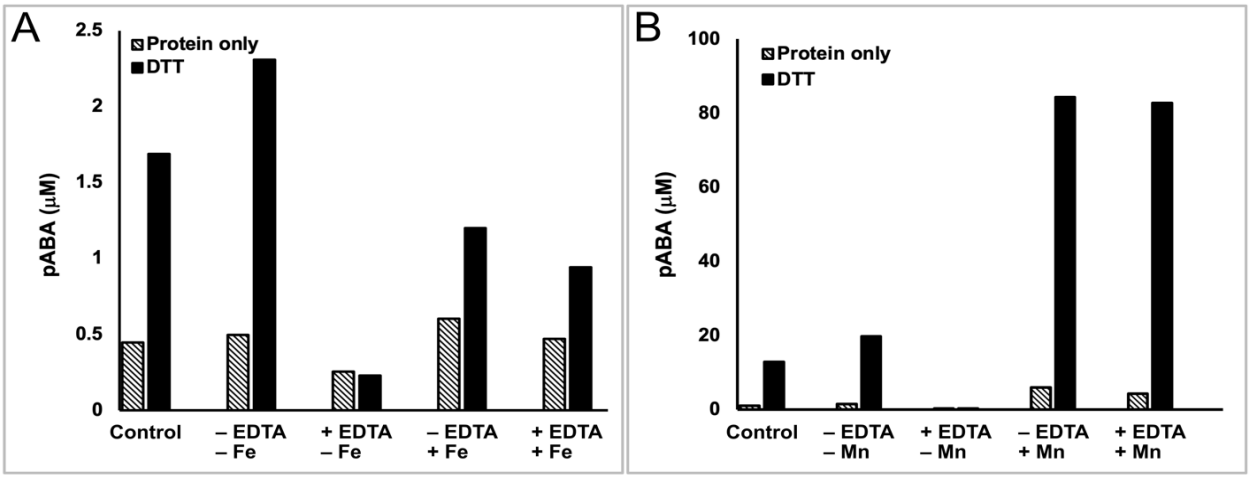

Figure 2.8 Restoring pABA synthase activity after incubating CT610 with EDTA to remove any present cofactors or bound pABA. A) EDTA experiments with Fe/Fe reconstitution. B) EDTA experiments with Mn/Mn reconstitution.

2.4.8 $^{18}O_2$ experiments

Since CT610 showed the greatest amount of pABA produced when the protein was reconstituted with Mn, we decided to incubate reduced Mn-reconstituted CT610 in the presence of $^{18}O_2$ to elucidate how many oxygen atoms were being incorporated into the CT610-synthesized pABA molecule. The pABA produced by Mn-reconstituted CT610 exposed to regular $^{16}O_2$ displayed a $[M + H]^+$ ion at 138 m/z showing that only $^{16}O_2$ was incorporated (Figure 2.9A). Interestingly, the pABA produced by Mn-reconstituted CT610 exposed to $^{18}O_2$ displayed a $[M + H]^+$ ion at 142 m/z, showing CT610 incorporates two oxygen atoms from molecular oxygen into the resulting pABA molecule (Figure 2.9B). This supports our proposed mechanism where CT610 utilizes two monooxygenase reactions to produce the carboxylic acid portion of pABA.

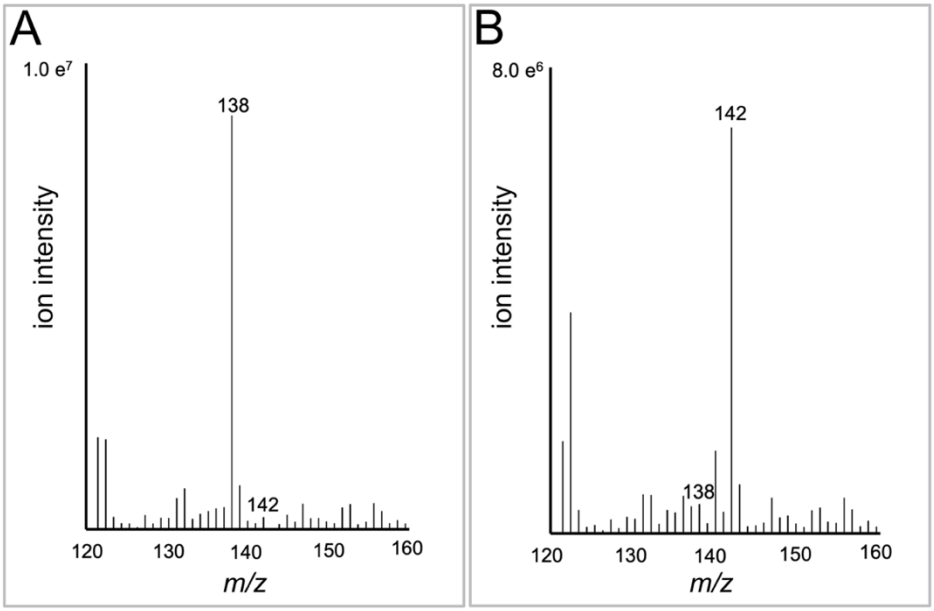

Figure 2.9 $^{18}O_2$ incorporation into pABA by Mn-reconstituted CT610. A) MS spectrum of pABA produced by reduced Mn-reconstituted CT610 using $^{16}O_2$ from injecting air into the anaerobic reactions. B) MS spectrum of pABA produced by reduced Mn-reconstituted CT610 using $^{18}O_2$.

2.4.9 MS experiments to identify potentially modified active site residues

Since we propose that CT610 uses its own active site residue(s) for pABA synthesis, we desired to determine whether any residues were modified after the reaction. Thus, we performed *in vitro* assays with as-purified CT610 compared to Mn-reconstituted CT610 and ran a portion of these reactions alongside controls on an SDS-PAGE gel (Figure 2.10). Interestingly, there is an extra band observed at ~25 KDa that is only present in the Mn-reconstituted reaction when reduced with DTT. This band could possibly be indicative of part of the CT610 backbone being cleaved during the reaction as the tyrosine residue is cleaved off. A portion of the bands were removed from the gel and the protein was digested with Glu-C protease followed by MS analysis. Preliminary MS analysis found one peptide with an unmodified Y27 residue suggesting this might not be the cleaved residue in this reaction. Unfortunately, no peptide containing the Y43 residue has been identified in preliminary experiments, thus we cannot conclude if this residue is modified/consumed in the reaction. Interestingly, a modified K152 residue was found to be aminoadipic acid, providing evidence that the amino group of this residue was removed to act as the amino donor in this reaction. Further analysis of the reacted vs. unreacted enzyme is currently underway.

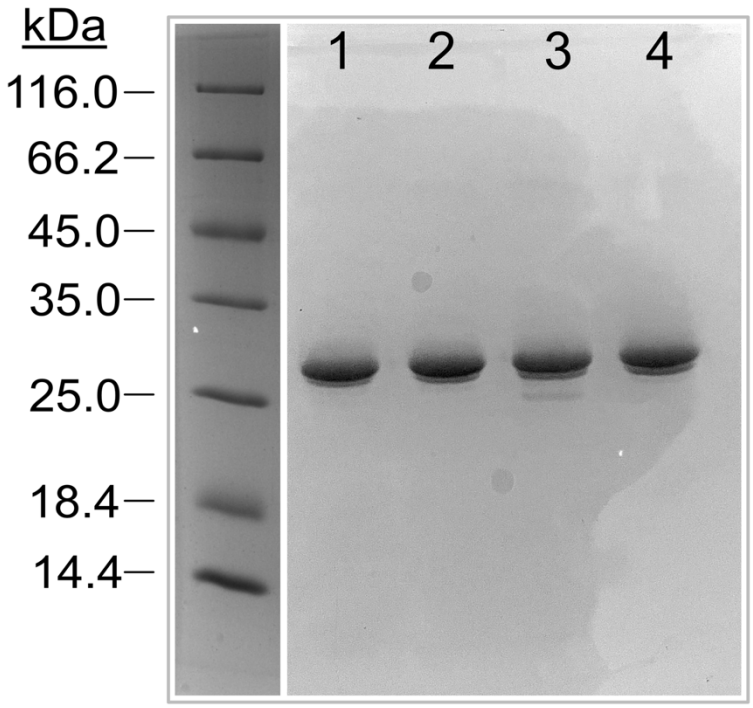

Figure 2.10 SDS-PAGE gel showing 4 μg of protein from each of the four reactions sent for MS analysis. 1 – non-reconstituted CT610 +DTT 2 – non-reconstituted CT610 protein only 3 – Mn-reconstituted CT610 +DTT 4 – Mn-reconstituted CT610 protein only.

2.5 Discussion

The biochemical characterization of CT610 reveals a unique enzyme involved in the *de novo* biosynthesis of folate in *C. trachomatis*. We propose that CT610 is a self-sacrificing enzyme that cleaves off a tyrosine residue to serve as a substrate for pABA biosynthesis[10]. Additionally, a conserved lysine residue, Lys152, may serve as the amino group donor in the reaction[10, 12]. Although residue-sacrificing enzymes have been previously documented, this mechanism is still rare and seems energetically costly to rely on[12-15]. Due to the essential nature of folate for the

growth of all cells, more information regarding the *de novo* biosynthesis of folate in *C. trachomatis* could possibly lead to novel antibiotics to treat chlamydial infections.

CT610 resembles nonheme diiron oxygenases that typically use their diiron active sites to complex with O_2 to cleave strong C–H or O–H bonds[9]. However, we show that CT610 pABA production is not stimulated by reconstitution with Fe^{II} but instead was increased ~90 fold when the enzyme was reconstituted with Mn^{II}. The pABA synthase activity of this enzyme is significantly decreased for the Y27F, Y43F, and K152R mutants showing that they are the most likely to be directly involved in the mechanism. These residues are relatively far from the diiron cofactor (6.6-14.6 Å) suggesting that Mn could be coordinated by different residues than the diiron site or some form of radical relay system is used to transfer the radical from the Mn metal center to the site of the pABA synthase reaction[10]. Protease digested Mn-reconstituted CT610 revealed a modified K152 residue that was missing the amino group, providing strong evidence that it was in fact the source of the amino group on the pABA molecule. Further, peptides containing unmodified Y27 residues were identified, without any sign of a potentially modified residue, suggesting it is not the cleaved residue.

2.5.1 Metal Cofactor

The first Fe-reconstitution was very promising since we saw a large increase in Fe content of the protein samples approaching the expected ratio, indicating that most of the protein contained the expected diiron cofactor. The drastic increase in oxygenase activity was similarly exciting as it showed the enzyme was consuming much more oxygen when the Fe cofactor was present, which was consistent with our proposed mechanism based off the O_2-activating mechanism of sMMO [10, 16]. However, it was shown that Fe is not required for CT610-catalyzed pABA

synthesis and instead the added iron seemed to inhibit pABA production. Based on the increase in activity in the presence of Mn, it is very likely that this reaction is Mn-dependent, thus somewhat contradicting the chemistry of our previously proposed mechanism and instead suggesting a mechanism more unique than we previously thought. It is unclear whether Mn binds to another region of the active site or if it replaces the Fe. Since the Mn-reconstituted protein did not consume nearly as much O_2 as the Fe-reconstituted protein and the Mn-reconstituted protein was shown to incorporate $^{18}O_2$ it is likely that the pABA synthase activity of this enzyme is entirely Mn-dependent and does not utilize a diiron cofactor to produce pABA. It is also worth mentioning that the Mn/Fe-reconstituted protein produced essentially the same amount of pABA as the Mn-reconstituted protein, showing that the addition of Fe does not significantly stimulate pABA production. The average pABA produced by reduced Mn-reconstituted CT610 is 34 μM per ~164 μM CT610. Since this is a proposed single-turnover self-sacrificing enzyme we would expect the ratio of product to enzyme to approach a 1:1 stoichiometric ratio of enzyme to product suggesting that approximately only 1/5 of the Mn-reconstituted enzyme is reacting in the *in vitro* reactions.

It is not uncommon for Mn to be involved in the chemistry of enzymes. Interestingly, the R2 subunit of class I RNR from *C. trachomatis* has a Mn/Fe center in place of the Fe/Fe center[17]. Potentially *C. trachomatis* prefers Mn/Fe cofactors over the traditional Fe/Fe cofactors. Mononuclear Mn^{II} is known to be used by glutamate synthetase as a Lewis acid catalyst[18, 19]. The class Ib ribonucleotide reductase from *E. coli* uses a dimanganese cofactor to activate the tyrosyl radical to produce deoxyribonucleotides[18, 20]. There are also several examples of nonheme mononuclear Mn^{II} enzymes such as Mn-dependent superoxide dismutase, oxalate oxidase and several others that showcase a wide variety of different mechanisms, with some employing an

active Mn^{II} cofactor while others use Mn^{III} in the active form of the enzyme[18, 21-25]. In the future, a crystal structure of Mn-reconstituted CT610 should be solved to determine where the metal is binding to further narrow down the type of mechanism that this enzyme employs to break strong C–H bonds and incorporate 2 oxygen atoms into pABA. It would also be interesting to see the EPR spectrum of anaerobic vs. aerobic Mn reconstituted CT610 to detect the presence of any radicals that might be produced. Currently there are no Mn-dependent self-sacrificing enzymes that have been characterized.

The fact that CT610 seems to be entirely Mn-dependent also prompts one to question the purpose of the diiron cofactor found in the crystal structure active site. ICP-AAS (Inductively coupled plasma atomic emission spectroscopy) analysis of purified CT610 revealed the enzyme had mostly iron with small amounts of zinc present in the protein leading to the conclusion that this enzyme contains a diiron active site[9]. CT610 is already known to be a moonlighting protein since it can both produce pABA and facilitate host cell apoptosis during chlamydial infection[6, 7]. It could be that the enzyme is using the diiron site to perform another function and either play a role in the mechanism of host cell apoptosis induction or possibly a third function currently unknown. Another possibility is that the diiron cofactor found in CT610 is mostly vestigial and there to support enzyme structure only, although our data would suggest that iron is not required for pABA production and so not essential for structural integrity. The increased oxygenase activity in Fe-reconstituted CT610 could have been due to the diiron active site reacting with oxygen unproductively, not producing pABA but instead reducing O_2 to H_2O_2. It is common in flavin monooxygenases to use their catalytic reactive peroxide intermediate to oxygenate their substrates as well as release H_2O_2 into solution when the substrate is either missing or in the wrong orientation in a process known as uncoupling[26].

2.5.2 Potential self-sacrificing residues

The CT610 ortholog from *N. europaea*, NE1434, has conserved tyrosine residues corresponding to Y27, Y43 and Y47, while Y141 and Y170 are naturally found as phenylalanine in the ortholog, suggesting that the tyrosine residue donated in this reaction is most likely either Y27, Y43 or Y47 if NE1434 and CT610 use the same mechanism to produce pABA (Figure 2.11). Similarly, NE1434 contains a conserved lysine residue corresponding to CT610 K152 that is proposed to be the amino group donor in this reaction (Figure 2.11). Previous work showed that the Y27F and Y43F active site variants had the most significant decrease in pABA production and we confirmed this variant pABA synthase activity[10]. This suggests that the tyrosine residue that is cleaved in CT610-catalyzed pABA biosynthesis can be further narrowed down to Y27 and Y43. Similarly, the K152R variant showed almost no pABA synthase activity suggesting this lysine residue is important in catalysis, potentially as the unknown amino donor. It is unclear why the Y27F, Y43F and K152R consumed more oxygen when reconstituted with iron, however this could similarly be due to an unproductive reaction of the metal cofactor and oxygen and be completely unrelated to pABA production.

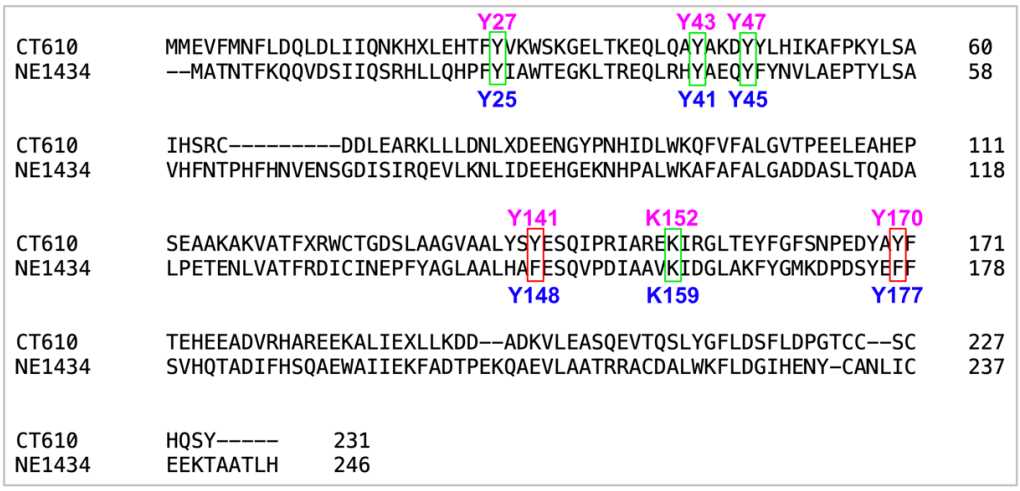

Figure 2.11 Sequence alignment comparing CT610 (Pink) and NE1434 (Blue) where key conserved residues are boxed in green and key residues that are not conserved are boxed in red.

Some samples of CT610 were sent for digested peptide MS analysis and we are currently submitting and analyzing further samples for this analysis. Interestingly, there was a small band with a lower molecular weight that was found when the Mn-reconstituted reacted protein was run on an SDS-PAGE gel, possibly suggesting that part of the peptide backbone of CT610 was cleaved along with the donated tyrosine residue producing a smaller peptide fragment. An unmodified Y27 residue was found on one peptide fragment in the reacted protein suggesting that this is not the cleaved residue, however it is possible that this fragment was from an unreacted protein molecule. Currently, a Y43 residue has not been identified from the digest of reacted CT610, which could suggest it is the residue that was cleaved off the protein and is missing altogether; however, this is also still not confirmed. Interestingly, a modified K152 residue was found to be converted to aminoadipic acid, which can easily occur via oxidation of the aldehyde that would be produced when the amino group is donated to produce the pABA molecule. Further analysis of the unreacted vs the reacted protein is currently under investigation.

Our proposed mechanism is heavily based on the hydroxylase component of sMMO where a highly reactive bis-μ-oxo-iron^{IV} Fe_2O_2 (Figure 2.12, red box) complex is used to oxidize the substrate, but instead of oxidizing methane with a diiron cofactor like sMMO the β-carbon of a tyrosine residue is oxidized by potentially a dimanganese cofactor allowing for cleavage of the residue from the backbone yielding *p*-hydroxybenzaldehyde and an Mn^{III}/ Mn^{III} cofactor[10, 16]. Another radical hydroxylation reaction occurs after the cofactor is re-reduced, producing *p*-hydroxybenzoate (pHB). This molecule is aminated, potentially using Lys152 as an amino group donor, then dehydrated and rearranged to produce the final pABA molecule (Figure 2.12).

Although there is still much unknown about how this enzyme synthesizes pABA, it is clear that this is a Mn-dependent enzyme that incorporates two atoms of oxygen into the molecule of pABA synthesized, thus highlighting CT610 as a novel self-sacrificing metallo-oxygenase required for folate biosynthesis *in C. trachomatis*.

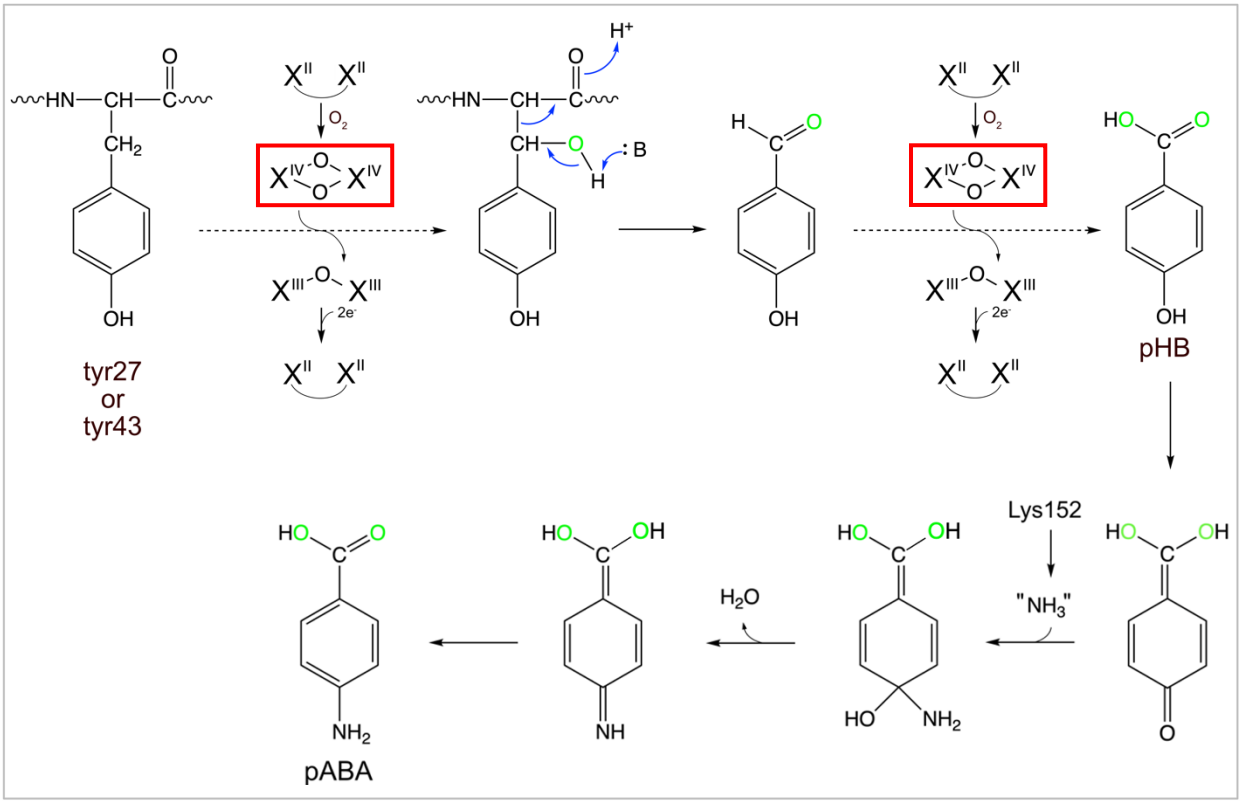

Figure 2.12 Proposed mechanism for CT610-derived pABA biosynthesis where CT610-incorporated oxygens are shown in green. The reactive cofactor intermediate is boxed in red.

2.6 Future Directions

In order to further elucidate the mechanism in which CT610 sacrifices its own tyrosine residue to produce pABA and therefore participate in *de novo* biosynthesis of pABA in *C. trachomatis*, the exact site where Mn binds to the protein must be determined. This could give insight to how many atoms of Mn are involved in the incorporation of the two oxygen atoms of the pABA molecule to further narrow down the mechanism of the sacrificial tyrosine cleavage. The crystal structure of Mn-reconstituted CT610 could provide the Mn-binding site. It could also be possible to narrow down Mn-binding sites computationally by searching for sequence binding motifs. It would also be useful to test if the Fe-reconstituted protein produces H_2O_2 and therefore uncouples from the main reaction like FMOs to determine the role if any of the diiron cofactor so it can be ruled out of participating in the mechanism.

More troubleshooting is required to further increase the pABA produced by Mn-reconstituted CT610 to near 1:1 stoichiometric yield to help the protease-digested MS analysis required to determine which tyrosine residue is sacrificed for the produced pABA molecule.

Further characterization of ortholog NE1434 could also help narrow down the cleaved residue by repeating the pABA synthase analysis of Y25F, Y41F, Y45F and K159R variants. NE1434 should be reconstituted with Fe^{II}, Cu^{II}, Zn^{II} and Mn^{II} to determine if a similar increase in pABA synthase activity is shown. Reduced Fe- and Mn-reconstituted NE1434 should both be incubated with $^{18}O_2$ to determine which reconstitution is responsible for the incorporation of oxygen into the resulting pABA molecule.

It would also be useful to investigate the pABA synthase activity of Y27A, Y27G, Y43A and Y43G variants and attempt to restore the likely decreased pABA synthase activity with the

addition of free *L*-tyrosine. This could suggest that any variant that increases in pABA synthase activity with the addition of free *L*-tyrosine is the site of the sacrificial tyrosine residue.

References:

[1] Green, J. M., and Matthews, R. G. (2007) Folate Biosynthesis, Reduction, and Polyglutamylation and the Interconversion of Folate Derivatives, *EcoSal Plus 2*.

[2] Adams, N. E., Thiaville, J. J., Proestos, J., Juárez-Vázquez, A. L., McCoy, A. J., Barona-Gómez, F., Iwata-Reuyl, D., de Crécy-Lagard, V., and Maurelli, A. T. (2014) Promiscuous and adaptable enzymes fill "holes" in the tetrahydrofolate pathway in Chlamydia species, *mBio 5*, e01378-01314.

[3] (2021) Chlamydia Statistics, https://www.cdc.gov/std/chlamydia/stats.htm.

[4] Cheong, H. C., Lee, C. Y. Q., Cheok, Y. Y., Tan, G. M. Y., Looi, C. Y., and Wong, W. F. (2019) Chlamydiaceae: Diseases in Primary Hosts and Zoonosis, *Microorganisms 7*.

[5] Zomorodipour, A., and Andersson, S. G. (1999) Obligate intracellular parasites: Rickettsia prowazekii and Chlamydia trachomatis, *FEBS Lett 452*, 11-15.

[6] Fan, H., Brunham, R. C., and McClarty, G. (1992) Acquisition and synthesis of folates by obligate intracellular bacteria of the genus Chlamydia, *J Clin Invest 90*, 1803-1811.

[7] de Crécy-Lagard, V., El Yacoubi, B., de la Garza, R. D., Noiriel, A., and Hanson, A. D. (2007) Comparative genomics of bacterial and plant folate synthesis and salvage: predictions and validations, *BMC Genomics 8*, 245.

[8] Stenner-Liewen, F., Liewen, H., Zapata, J. M., Pawlowski, K., Godzik, A., and Reed, J. C. (2002) CADD, a Chlamydia protein that interacts with death receptors, *J Biol Chem 277*, 9633-9636.

[9] Schwarzenbacher, R., Stenner-Liewen, F., Liewen, H., Robinson, H., Yuan, H., Bossy-Wetzel, E., Reed, J. C., and Liddington, R. C. (2004) Structure of the Chlamydia protein CADD reveals a redox enzyme that modulates host cell apoptosis, *J Biol Chem 279*, 29320-29324.

[10] Macias-Orihuela, Y., Cast, T., Crawford, I., Brandecker Kevin, J., Thiaville Jennifer, J., Murzin Alexey, G., de Crécy-Lagard, V., White Robert, H., Allen Kylie, D., and Metcalf William, W. (2020) An Unusual Route for p-Aminobenzoate Biosynthesis in Chlamydia trachomatis Involves a Probable Self-Sacrificing Diiron Oxygenase, *Journal of Bacteriology 202*, e00319-00320.

[11] Beinert, H. (1978) Micro methods for the quantitative determination of iron and copper in biological material, *Methods Enzymol 54*, 435-445.

[12] Sakaki, K., Ohishi, K., Shimizu, T., Kobayashi, I., Mori, N., Matsuda, K., Tomita, T., Watanabe, H., Tanaka, K., Kuzuyama, T., and Nishiyama, M. (2020) A suicide enzyme catalyzes multiple reactions for biotin biosynthesis in cyanobacteria, *Nat Chem Biol 16*, 415-422.

[13] Chatterjee, A., Abeydeera, N. D., Bale, S., Pai, P. J., Dorrestein, P. C., Russell, D. H., Ealick, S. E., and Begley, T. P. (2011) Saccharomyces cerevisiae THI4p is a suicide thiamine thiazole synthase, *Nature 478*, 542-U146.

[14] Desguin, B., Soumillion, P., Hols, P., and Hausinger, R. P. (2016) Nickel-pincer cofactor biosynthesis involves LarB-catalyzed pyridinium carboxylation and LarE-dependent sacrificial sulfur insertion, *Proc Natl Acad Sci U S A 113*, 5598-5603.

[15] Lai, R. Y., Huang, S., Fenwick, M. K., Hazra, A., Zhang, Y., Rajashankar, K., Philmus, B., Kinsland, C., Sanders, J. M., Ealick, S. E., and Begley, T. P. (2012) Thiamin pyrimidine

biosynthesis in Candida albicans : a remarkable reaction between histidine and pyridoxal phosphate, *J Am Chem Soc 134*, 9157-9159.
[16] Ross, M. O., and Rosenzweig, A. C. (2017) A tale of two methane monooxygenases, *J Biol Inorg Chem 22*, 307-319.
[17] Jiang, W., Yun, D., Saleh, L., Barr, E. W., Xing, G., Hoffart, L. M., Maslak, M. A., Krebs, C., and Bollinger, J. M., Jr. (2007) A manganese(IV)/iron(III) cofactor in Chlamydia trachomatis ribonucleotide reductase, *Science 316*, 1188-1191.
[18] Zhu, W., and Richards, N. G. J. (2017) Biological functions controlled by manganese redox changes in mononuclear Mn-dependent enzymes, *Essays Biochem 61*, 259-270.
[19] Wedler, F. C., Denman, R. B., and Roby, W. G. (1982) Glutamine synthetase from ovine brain is a manganese(II) enzyme, *Biochemistry 21*, 6389-6396.
[20] Cotruvo, J. A., Jr., and Stubbe, J. (2010) An active dimanganese(III)-tyrosyl radical cofactor in Escherichia coli class Ib ribonucleotide reductase, *Biochemistry 49*, 1297-1309.
[21] Borgstahl, G. E., Parge, H. E., Hickey, M. J., Beyer, W. F., Jr., Hallewell, R. A., and Tainer, J. A. (1992) The structure of human mitochondrial manganese superoxide dismutase reveals a novel tetrameric interface of two 4-helix bundles, *Cell 71*, 107-118.
[22] Requena, L., and Bornemann, S. (1999) Barley (Hordeum vulgare) oxalate oxidase is a manganese-containing enzyme, *Biochem J 343 Pt 1*, 185-190.
[23] Tanner, A., Bowater, L., Fairhurst, S. A., and Bornemann, S. (2001) Oxalate decarboxylase requires manganese and dioxygen for activity. Overexpression and characterization of Bacillus subtilis YvrK and YoaN, *J Biol Chem 276*, 43627-43634.
[24] Whiting, A. K., Boldt, Y. R., Hendrich, M. P., Wackett, L. P., and Que, L., Jr. (1996) Manganese(II)-dependent extradiol-cleaving catechol dioxygenase from Arthrobacter globiformis CM-2, *Biochemistry 35*, 160-170.
[25] Hamberg, M., Su, C., and Oliw, E. (1998) Manganese lipoxygenase. Discovery of a bis-allylic hydroperoxide as product and intermediate in a lipoxygenase reaction, *J Biol Chem 273*, 13080-13088.
[26] Catucci, G., Gao, C., Rampolla, G., Gilardi, G., and Sadeghi, S. J. (2019) Uncoupled human flavin-containing monooxygenase 3 releases superoxide radical in addition to hydrogen peroxide, *Free Radic Biol Med 145*, 250-255.